



# Metallomics

**Iron deficiency and the loss of chloroplast iron-sulfur cluster assembly trigger distinct transcriptome changes in Arabidopsis rosettes**

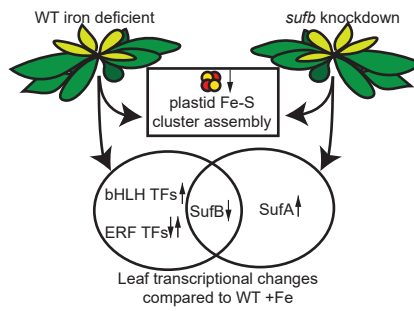
Journal:	<i>Metallomics</i>
Manuscript ID	MT-ART-07-2020-000175.R1
Article Type:	Paper
Date Submitted by the Author:	04-Sep-2020
Complete List of Authors:	Kroh, Gretchen; Colorado State University, Biology Pilon, Marinus; Colorado State University, Biology

SCHOLARONE™  
Manuscripts

### Significance to Metalloomics

Photosynthetic organisms have an exceptionally high iron (Fe) requirement. SufB, a protein required for chloroplast Fe-S cluster assembly is down-regulated early in response to low Fe in plants and cyanobacteria. The conserved down-regulation of SufB under Fe deficiency suggests an important physiological role. A comparison of the transcriptome for a SUFB knockdown mutant and a low Fe treatment in *Arabidopsis*, indicated distinct transcriptional responses despite displaying similar physiology and impaired photosynthesis. SufB loss caused transcriptome changes more reminiscent of Fe excess than deficiency. The data indicate that Fe deficiency and not Fe use triggers regulation of chloroplast Fe protein expression.

1 Graphic:



Text:

While a *sufB* knockdown mutant is phenotypically similar to wild-type (WT) Fe deficient plants, the leaf transcriptional response is distinct.

## ARTICLE

## Iron deficiency and the loss of chloroplast iron-sulfur cluster assembly trigger distinct transcriptome changes in Arabidopsis rosettes

Gretchen Elizabeth Kroh,<sup>\*a</sup> Marinus Pilon<sup>a</sup>

Received 00th January 20xx,  
Accepted 00th January 20xx

DOI: 10.1039/x0xx00000x

Regulation of mRNA abundance revealed a genetic program for plant leaf acclimation to Fe limitation. The transcript for SUFB, a key component of the plastid iron-sulfur (Fe-S) assembly pathway is down-regulated early after Fe deficiency, and prior to down-regulation of mRNAs encoding abundant chloroplast Fe containing proteins, which should economize the use of Fe. What controls this system is unclear. We utilized RNA-seq aimed to identify differentially expressed transcripts that are co-regulated with SUFB after Fe deficiency in leaves. To distinguish if lack of Fe or lack of Fe-S cofactors and associated loss of enzymatic and photosynthetic activity trigger transcriptome reprogramming, WT plants on low Fe were compared with an inducible *sufb*-RNAi knockdown. Fe deficiency targeted a limited set of genes and predominantly affected transcripts for chloroplast localized proteins. A set of glutaredoxin transcripts was concertedly down-regulated early after Fe deficiency, however when these same genes were down-regulated by RNAi the effect on known chloroplast Fe deficiency marker proteins was minimal. In promoters of differentially expressed genes, binding motifs for AP2/ERF transcription factors were most abundant and three AP2/ERF transcription factors were also differentially expressed early after low Fe treatment. Surprisingly, Fe deficiency in a WT on low Fe and a *sufb*-RNAi knockdown presented very little overlap in differentially expressed genes. *sufb*-RNAi produced expression patterns expected for Fe excess and up-regulation of a transcript for another Fe-S assembly component not affected by low Fe. These findings indicate that Fe scarcity, not Fe utilization, triggers reprogramming of the transcriptome in leaves.

### Introduction

In plants iron (Fe) is required as a cofactor in plastids for photosynthetic electron transport<sup>1</sup>, chlorophyll biosynthesis<sup>2</sup>, nitrogen (N)<sup>3</sup> and sulfur (S) assimilation<sup>4</sup>, NAD(P) synthesis<sup>5</sup> and reactive oxygen species (ROS) scavenging.<sup>6</sup> Outside of plastids important cofactor roles of Fe include mitochondrial metabolism,<sup>7</sup> as well as plant hormone synthesis (ABA and Auxin) and DNA metabolism.<sup>8</sup>

Three kinds of Fe cofactors exist in plants, non-heme iron, heme and siroheme (the latter only found in chloroplasts) and iron-sulfur (Fe-S) clusters which are the most abundant and versatile Fe cofactor.<sup>8</sup> In microbes just a few cases are reported where Fe cofactor requiring proteins are functionally replaced by proteins using alternative cofactors such as Cu (plastocyanin for cytochrome-*c*<sub>6</sub><sup>9–11</sup>) or flavin groups,<sup>12</sup> and MnSOD for FeSOD.<sup>13</sup> In higher plants, no firm evidence exists for functional replacement of Fe proteins albeit superoxide dismutase (SOD) activity in the chloroplast stroma can be provided by FeSOD isozymes as well as a Cu/ZnSOD.<sup>14</sup> The two least abundant FeSOD peptides (FSD2/3) form a dimer that is essential in

Arabidopsis.<sup>15</sup> Expression of the most abundant FeSOD (FSD1) and of CuZnSOD (CSD2) in the stroma is predominantly controlled by Cu status<sup>16–18</sup>. The inability to replace Fe enzymes underscores the unique and essential properties of Fe cofactors.<sup>8</sup>

Fe deficiency is common in plants because soil Fe is predominantly found in the ferric form, which is not readily available for uptake. To minimize negative impacts for growth and reproduction plants can acclimate to Fe deficiency with multiple strategies.<sup>19</sup> Plants can (1) induce more efficient mechanisms for uptake of Fe from the soil into the root with sustained export to the shoot,<sup>20,21</sup> (2) remodel metabolism to become less dependent on Fe<sup>22,23</sup> and (3) economize Fe to prioritize the use of Fe for specific functions over others.<sup>24</sup> The concept called Fe economy was used to describe the acclimation to low Fe of a member of the eukaryotic algae called *Chlamydomonas reinhardtii*.<sup>25</sup> In plants, Fe economy can be of great importance in the green leaf because of the exceptionally high Fe requirement of photosynthesis where one photosynthetic electron transport chain requires at least 24 Fe atoms.<sup>1</sup> Indeed, during Fe deficiency in Arabidopsis, photosynthesis is the process that is primarily affected.<sup>24,26</sup> Root Fe uptake is now very well characterized and is regulated both transcriptionally and post transcriptionally.<sup>27</sup> When Fe deficient, dicot plants such as Arabidopsis increase root Fe uptake.<sup>27–29</sup> Root Fe uptake machinery is up-regulated during low Fe via a cascade of Basic Helix Loop Helix (bHLH)

<sup>a</sup> Biology Department, Colorado State University, 2515 W. Pitkin Street, Fort Collins, CO 80523-1878.

\*Corresponding Author. Email: gkroh@colostate.edu

Electronic Supplementary Information (ESI) available: S. Figure 1, S Table 1, S. Table 2. See DOI: 10.1039/x0xx00000x

transcription factors (TF).<sup>30–33</sup> Recently, some members of the Ethylene Response Transcription Factor (ERF) family have also been linked to regulation of root and systemic Fe deficiency.<sup>34–36</sup> The master regulator of the root Fe uptake machinery, Fer Like Iron Deficiency Induced Transcription factor (FIT), is stabilized during Fe deficiency by the ERF transcription factors, Ethylene Insensitive 1 (EIN1) and Ethylene Insensitive 1 Like 3 (EIL3).<sup>34</sup> ERF4 and ERF72 both negatively regulate IRT1 expression in the roots, but also directly bind the promoter of the chlorophyll degradation gene *AtCLH1* and have been suggested to positively regulate chlorophyll degradation during Fe deficiency.<sup>37,38</sup>

Relative to root Fe uptake our understanding of metabolic remodeling and Fe economy in leaves is limited.<sup>19</sup> Fe deficiency in the leaf results in reduced abundance of several Fe proteins and is associated with impaired photosynthesis.<sup>22,23</sup> Transcriptome and proteome changes that indicate remodeling in *Arabidopsis* include decreased chlorophyll synthesis, changes in expression of ROS scavenging molecules, decreased expression of photosynthetic proteins, and altered amino acid assimilation.<sup>23,26,39,40</sup> In the *Arabidopsis* Fe economy response, the leaf apparently prioritizes mitochondrial function over that of the chloroplast,<sup>24</sup> which normally contains about 80% of leaf Fe.<sup>41</sup> Not all Fe proteins are affected to the same extent by Fe deficiency treatment as specific chloroplast located iron-sulfur (Fe-S) cluster proteins, notably ferredoxin (FDX) and the Rieske subunit of the cytochrome-*b<sub>6</sub>f* (Cyt-*b<sub>6</sub>f*) complex were especially affected early after deficiency which may help to increase Fe for prioritized pathways such as respiration in the mitochondria.<sup>24</sup> The diminished abundance on low Fe of normally highly expressed Fe proteins is in a large part due to transcript level regulation indicating the presence of a genetic program that helps acclimate leaves to Fe limitation. Interestingly, the transcript for *SUFB*, a key component of the plastid Fe-S assembly pathway is also down-regulated early after Fe deficiency treatment is started, and even prior to the down-regulation of mRNAs encoding abundant chloroplast Fe containing proteins. Remarkably, the down-regulation of *SUFB* transcript during Fe deficiency is conserved from plants<sup>23,24,42–44</sup> to cyanobacteria<sup>45</sup> suggesting this is an important acclimation needed for either economical use of Fe or the prevention of accumulation of potentially toxic incomplete cofactors in diverse photosynthetic organisms.

SUF-mediated Fe-S assembly in plastids begins with the two-component cysteine desulfurase, made up of a protein called CpNIFS, which is now called SUFS, together with the SUFE1 protein. The SUFS/SUFE1 complex serves to efficiently remove a S atom from cysteine, an essential function.<sup>46–48</sup> The S is subsequently incorporated into an Fe-S cluster on the SUFBCD major assembly scaffold.<sup>49</sup> Finally, transfer proteins in the SUF pathways help with maturation and insertion of Fe-S clusters into required proteins. The strongest evidence for function as plastid Fe-S transfer proteins is provided for the three NFU proteins<sup>50,51</sup> and for HCF101<sup>52</sup> as *Arabidopsis* knockout lines of any of these proteins exhibit defects in maturation of specific Fe-S requiring proteins.<sup>50–52</sup> Other candidate Fe-S transfer proteins include SUFA<sup>53</sup>, and Monothiol Glutaredoxins.<sup>54</sup> The

SUF pathway is required for maturation of all Fe-S containing photosynthetic electron transport proteins in plants.<sup>55</sup> In dexamethasone (DEX) inducible *sufb*-RNAi knockdown lines, all Fe-S containing photosynthetic proteins were decreased in accumulation after RNAi induction.<sup>55</sup> Thus, the induced *sufb*-RNAi knockdown in plants grown on regular Fe-replete soil results in symptoms at the protein accumulation level reminiscent of chloroplast Fe deficiency.<sup>55</sup> However, with mild Fe deficiency, the Cyt-*b<sub>6</sub>f* complex and FDX2 are down-regulated early, but Fe requiring subunits of Photosystem-I (PSI) remained abundant.<sup>24</sup> In this regard, mild Fe deficiency and lack of SUFB differ in their effects on PSI while in both cases the Cyt-*b<sub>6</sub>f* complex and FDX protein level are severely decreased.

While class IV bHLH TFs, IRL3/bHLH105, PYE, and class 1b bHLH TFs, bHLH101, bHLH100 which are linked to regulation of root Fe homeostasis are expressed also in the shoots and induced by Fe deficiency,<sup>23,56,57</sup> nucleus encoded chloroplast factors that seem to be regulated for Fe-economy, such as *SUFB*, have no putative bHLH *cis* elements in the promoter, and *FDX2* has only one bHLH *cis* elements in the promoter.<sup>24</sup> Thus, so far undiscovered mechanisms of regulation must be required to initiate changes to chloroplast proteins during Fe deficiency. How the leaf coordinates adjustment of its transcriptome to low Fe and what triggers such a response is still largely unclear. We employed an RNA-seq approach to identify differentially expressed transcripts that are co-regulated early after Fe deficiency treatment. A lack of Fe cofactor assembly inevitably results in limited enzymatic and photosynthetic activity in plastids, which can potentially cause feed back into gene expression that governs chloroplast biogenesis. We therefore compared differentially expressed genes (DEGs) in WT rosettes of plants on low Fe with an inducible *sufb*-RNAi knockdown line in order to help identify if lack of Fe per se or lack of Fe-S cofactors and associated loss of enzymatic activity and photosynthetic electron transport trigger the reprogramming of the transcriptome. The findings indicate that Fe deficiency and not chloroplast Fe utilization is a direct trigger for the reprogramming of the transcriptome in leaves, but the nuclear encoded chloroplast localized transcripts are early targets of Fe deficiency.

## Materials and Methods

**Plant lines.** Wild type *Arabidopsis* ecotype Col-0 was used as a control line. The Dexamethasone (DEX) inducible RNAi knockdown mutants *sufb1-12*, *sufb2-2*, *sufc2-10-2*, and *sufd2-13* were a gift from Dr. Ryouichi Tanaka (Hokkaido University, Sapporo, Japan) and are described in Hu *et al.* (2017). Knockout lines for *sufa1-2* (Salk 147938C) were obtained from the Arabidopsis Biological Resource Center (Ohio State University) and genotyped by PCR (*SufA* specific primers: 5' AAATCAGCCAAAAGAGAGGCC 3', 5'GAATATCTCAGCTGCACCTGC 3'; TDNA left boarder primer: 5' ATTTTGCCGATTCGGAAC 3'). RNAi lines of *grsx 3,4,5,7,8* were a gift from Dr. Matthew Escobar (California State University, San Marcos) and are described.<sup>58,59</sup>

**Plant growth and sampling.** The *sufb*, *sufc*, and *sufd*-RNAi lines were grown alongside Col-0 hydroponically.<sup>60</sup> The *sufb*, *sufc*, and *sufd*-RNAi lines were maintained on sufficient Fe conditions (10  $\mu$ M Fe(III)EDTA). To induce Fe deficiency in Col-0, plants that were four weeks old (10–14 leaf stage) were transferred to 1/5<sup>th</sup> Hoagland's supplemented with 10 nM Fe(III)EDTA, whereas control groups were maintained at 10  $\mu$ M Fe(III)EDTA.<sup>24</sup> All experiments were done with at least 3 biological replicates and samples were taken from three growth rounds of the plants.

For RNA-sequencing, we used three groups of plants as treatments: WT on sufficient Fe (**WT +Fe, control**), WT on low Fe (**WT – Fe, treatment**), and inducible *sufb*-RNAi on +Fe (***sufb*-RNAi +Fe**). For RNAi, *sufb2-2* was chosen as a representative line because it had one of the strongest phenotypic responses and change in SUFB protein accumulation when grown on soil<sup>55,61</sup> and hydroponics (data not shown). 26 days after stratification, all *sufb2-2* and Col-0 hydroponically grown plants were foliar sprayed on their rosettes only in a chemical fume hood with 15  $\mu$ M DEX (Dexamethasone- Cyclodextrin complex; Sigma Aldrich, St. Louis MO) in 0.02% tween (v/v) (Bio-Rad, Hercules, CA) to ensure induction of the RNAi transcript. WT plants did not present any visible effects of DEX treatment and SUFB, along with other Fe responsive proteins, were unaffected by DEX treatment in the WT as judged by Western blotting (not shown). Two days later at 4 weeks of age, half of the Col-0 plants were transferred to low Fe (Figure 1a) at the start of the light cycle. Samples of WT +Fe control, WT -Fe treatment and *sufb2-2* (*sufb*-RNAi +Fe), for RNA sequencing were taken at 2 h (time point (TP A)) and 26 h (TP B) after Col-0 was transferred to low Fe, corresponding to 2 h after the start of the light cycle to avoid circadian effects. TP A was 2 days after DEX treatment, and TP B was 3 days after DEX treatment. All sampling was done 2 h after the onset of the light period. Three whole rosettes were pooled into one biological replicate and 3 biological replicates were sequenced. Samples were also taken for protein analysis at TP B and 7 days after low Fe treatment and 9 days after DEX treatment (TP C). For all other experiments with *sufb*, *sufc*, and *sufd* lines, plants were foliar sprayed with 10  $\mu$ M DEX in 0.02% tween (v/v) which was determined to be sufficient for RNAi induction.<sup>55,61</sup>

**RNA-sequencing.** Rosette samples from three biological replicates for each treatment were flash frozen in liquid nitrogen for RNA-sequencing. Tissue was homogenized using a Qiagen Tissue Lyser and RNA was isolated using a Qiagen RNeasy Plant Mini Kit (Qiagen; Hilden, Germany). RNA quality was assessed by an Agilent TapeStation 4200 using a high sensitivity RNA screen tape and RNA samples with an RNA integrity number (RIN) of >5 were sequenced. RNA quantity was measured with a Qubit 2.0 Fluorometer using a broad range assay kit and between 1.0 and 1.9  $\mu$ g RNA of each sample was shipped on dry ice to Novogene Corp. (Davis, CA) for library preparation and RNA-sequencing. Library preparation was done using poly-A selection for nuclear encoded mRNA at Novogene. cDNA was sequenced using Illumina at a depth of 150 paired end reads for a sequencing coverage of at least 55 x 10<sup>6</sup> reads per sample.

**Bioinformatic analysis.** High quality reads were trimmed to remove adapter sequences at Novogene. Reads were discarded when uncertain bases composed >10% (N>10%) of the read and when base quality of less than a Phred score of 20 constituted more than 50% of the read. Trimmed reads were then aligned and mapped to the TAIR10 genome using HISAT2 2.1.0 beta<sup>62</sup> and FPKM values were calculated using HTseq v0.6.1.<sup>63</sup> Differential expression was determined using DESeq version 1.10.1 and p-value was adjusted using Bonferroni adjustment. The differential expression threshold was set at a fold change of 1.5x and an adjusted p-value of less than 0.05. Differential expression at each time point between relevant pairs of treatments were compared using Interactienn.<sup>64</sup>

Putative transcription factor binding sites were identified in promoter sequences of differentially expressed genes (DEGs) at TP B in AthaMap ([http://www.athamap.de/search\\_gene.php](http://www.athamap.de/search_gene.php)<sup>65</sup>). Promoter region was set to 1000 bp upstream of the start site of transcription. To determine if specific *cis* elements were enriched in the DEGs relative to the rest of the genome, we used the TAIR Motif Search (<https://www.arabidopsis.org/tools/bulk/motiffinder/index.jsp>). Promoter region was set to 1000 bp upstream of the start of transcription and *cis* elements were only reported if they occurred more than 3 times in a promoter. Enrichment of *cis* elements was determined if the probability of motif occurrence in DEG promoters was significantly higher than the probability of motif occurrence across the *Arabidopsis* genome (p<0.05). *Cis* elements analyzed were as follows: the E-Box for bHLH (CANNTG<sup>66</sup>), and the GCC-Box for ERF (GCCGCC<sup>67</sup>).

**Gene expression analysis via qRT-PCR.** For gene expression (mRNA level) analysis of hydroponically grown plants using qRT-PCR, three rosettes were pooled for one biological replicate, and 3 biological replicates were analyzed. For gene expression analysis of seedlings grown on plates, 10 shoots were pooled for one biological replicate and 3-4 biological replicates were analyzed. Tissue was homogenized using a Qiagen tissue lyser and RNA was isolated using the TRIzol extraction method (Life Technologies;<sup>60</sup>). 2  $\mu$ g of RNA was treated with 12 U DNase I (Invitrogen, Carlsbad, CA) and cDNA was synthesized using a superscript III cDNA synthesis kit (Invitrogen, Carlsbad, CA). For qPCR, each biological replicate was run in two technical replicates. A second RNA sample from each biological replicate was treated with DNase I only, to serve as a -RT control. Gene expression (relative transcript abundance) was normalized to expression of *Ubiquitin 10* (*UBQ10*) and then to the level of gene expression of WT +Fe control using the  $\Delta\Delta$ CT method.<sup>68</sup> All primers were tested for 95% efficiency or better and were designed according to Udvardi *et al.*<sup>69</sup> and are listed in Kroh and Pilon.<sup>60</sup>

**Protein analysis.** Three rosettes per sample for hydroponically grown plants and 10 shoots per sample of plate grown seedlings were pooled for protein analysis. At least 3 biological reps were analyzed. Total protein was extracted and western blotting was carried out as described in Kroh and Pilon.<sup>60</sup> Primary antibodies

for FDX, *Cytf*, *Cytb<sub>6</sub>*, Rieske, Photosystem-I subunit A (PSaA), and Cytosolic fructose-1,6-bisphosphatase (cFBpase) were obtained from Agrisera (Vannas, Sweden). Primary antibody for SUFB was a gift from Dr. Nicolas Rouhier (Université de Lorraine, Nancy, France). Detection of secondary antibodies was by alkaline phosphatase (Sigma Aldrich, St. Louis, MO). For protein quantification, a dilution series of a WT +Fe control was included. Blot images were scanned into a computer to generate a TIFF file and then intensity of bands was measured using Image Studio Lite by LiCor (Lincoln, NE) and a standard curve was generated to compare intensity of other samples from the same gel.

**Elemental Analysis.** Shoot elemental analysis was analyzed at TP C for hydroponic experiments. Two rosettes were pooled for one biological replicate and tissue was dried at 60°C for two weeks and then digested in HNO<sub>3</sub>.<sup>70</sup> Digested samples were resuspended in 1% HNO<sub>3</sub> and analyzed on an ICP-OES. Concentration of elements in each sample was normalized by dry weight. At least 7 biological reps of each treatment were analyzed.

**Ferric Chelate Reductase Activity.** Root Fe reductase activity was measured at TP C according to Grusak.<sup>71</sup> One whole root system was measured per replicate. Roots were excised from the plant and were rinsed twice with 1/5<sup>th</sup> strength Hoagland's solution without Fe to rinse off Fe from the hydroponic solution. Roots were then transferred to the assay solution which contained 1/5<sup>th</sup> Hoagland's, 100 μM Fe(III)EDTA and 100 μM bathophenanthrolinedisulfonic acid (BPDS). After 30 minutes in the assay solution, roots were removed, patted dried and weighed. The absorbance of the assay solution was measured at 535 nm and used to calculate the reductase activity. Reductase activity was calculated on a root fresh weight basis. At least 5 root systems per treatment were analyzed.

**Chlorophyll Fluorescence.** Chlorophyll fluorescence was measured to assess photosynthetic capacity of plants at TP C. False color images were taken using a FluorCam in Quenching Analysis setting (Photo Systems Instruments, Brno, Czech Republic). A whole *Arabidopsis* plant was used for measurements and measurements were taken under a light intensity of 100 μmol m<sup>-2</sup> s<sup>-1</sup>. Plants were dark adapted for 30 min<sup>24</sup> and  $\phi$ PSII was calculated according to Maxwell and Johnson.<sup>72</sup>

**Statistical Analysis.** A 2 factor ANOVA was run in R version 3.4.4 to determine differences between treated and control plants (p value <0.05). A Tukey test was used to determine which treatment groups were significant in the ANOVA using the lsmeans R package. Data visualization was done using Sigma Plot version 7.4 and BioVinci version 1.15.

## Results

**Experimental strategy for RNA-seq.** We aimed to analyze the early effects of transfer to low Fe on differential gene

expression in rosettes of WT plants and for reference made a comparison with an induced *sufb*-RNAi line. *Sufb2-2* plants were maintained on sufficient levels of Fe for the duration of the experiment. Before RNAi induction, these plants were phenotypically the same as WT, as expected.<sup>55</sup> To induce the *sufb*-RNAi knockdown construct the rosettes of inducible *sufb2-2*-RNAi plants were sprayed with DEX at 26 days after germination. For control, all WT rosettes were also sprayed with DEX at the same time, which did not cause any visible symptoms in WT plants (Figure 1). When plants were at 4 weeks of age, exactly two days after DEX treatment and at the start of the light period, which we designated T=0, half of the WT plants were transferred to low Fe (10 nM Fe(III)EDTA) (**WT -Fe, treatment**), while the other half of WT plants (**WT +Fe, control**) and all *sufb2-2*-RNAi plants (***sufb*-RNAi +Fe**) were maintained at sufficient iron (10 μM Fe(III)EDTA). Samples were taken for RNA extraction of all three treatment groups at 2 h after the WT -Fe treatment had been transferred to low Fe (TP A) and exactly one day later, at 26 h (TP B) (Figure 1a). For further controls, samples to measure protein accumulation were also taken at TP B and 7 days + 2 h after WT -Fe treatment at TP C (Figure 1a). We timed all sampling to be at 2 h after the start of the light period in order to minimize the effects of circadian rhythm.<sup>73</sup>

**Comparison of symptoms and phenotypes.** We first compared the symptoms resulting from low Fe treatment (WT -Fe treatment relative to the WT +Fe control) with the effect of induced loss of SUFB by RNAi (*sufb*-RNAi +Fe relative to the WT +Fe control). There were no noticeable developmental differences between the WT plants before the start of Fe deficiency treatment and *sufb*-RNAi +Fe, which at that point were at two days into induction of RNAi (Figure 1b). However, by TP B, at 4 days after RNAi induction, chlorosis was observed in the young leaves of *sufb*-RNAi +Fe (Figure 1b). *SUFB* transcript level was verified to be decreased in *sufb*-RNAi +Fe at TP A and TP B as expected, and the *SUFB* transcript level of WT -Fe treatment matched that of *sufb*-RNAi +Fe at TP B (Figure 1c). *SUFB* protein accumulation was also assessed in all treatments at TP B via western blotting before samples were sent for RNA sequencing. *SUFB* protein accumulation was lower in *sufb*-RNAi +Fe plants compared to both WT +Fe control (as expected) and WT -Fe treatment at TP B (Figure 1d, e). While *SUFB* mRNA was down-regulated early after Fe deficiency in the WT -Fe treatment, decreases in *SUFB* protein accumulation were expected to be minimal in the first days after transfer to low Fe.<sup>24</sup> Therefore, *SUFB* protein accumulation was also measured at TP C to ensure that the WT -Fe treatment ultimately resulted in low *SUFB* protein accumulation. Indeed, whole rosette *SUFB* protein accumulated to low levels in WT -Fe treatment after 7 days of deficiency and matched that of *sufb*-RNAi +Fe (Figure 1d, e). These data indicate that physical symptoms in response to *sufb*-RNAi +Fe and WT -Fe were similar and the two treatments accumulated similar levels of *SUFB* protein and transcript.

**Overview of RNA-sequencing coverage.** For RNA-sequencing, three independent biological replicates, comprised of three

whole rosettes, for each WT -Fe treatment, WT +Fe control, and *sufb-RNAi* +Fe were sequenced at TP A and TP B. The number of raw reads per sequenced sample ranged from 61 million reads to 100 million reads (S. Table 1). Clean reads on average made up 97% of the raw reads/sample (S. Table 1). The Q20 score, indicating the percentage of bases that were correctly recognized > than 99% of the time, was above 98% for all reads, suggesting that the incorrect base calling rate was low (S. Table 1). Within each group (WT +Fe control, WT -Fe treatment, *sufb-RNAi* +Fe) at each time point, correlation between biological replicates was high, with a Pearson correlation coefficient of above .98 for each group (data not shown). Reads from biological replicates within each treatment had minimal variation in gene expression. Differential expression was determined using an adjusted p-value of >0.05 and a fold change of +/- 1.5 from WT +Fe.

**WT -Fe treatment and *sufb-RNAi* +Fe present distinct transcriptional changes.** Overall, transcriptional changes in WT -Fe treatment and *sufb-RNAi* +Fe were minimal when both were compared to the WT +Fe control (Figure 2) with only 86 and 147 DEGs present at respectively TP A and TP B in WT -Fe treatment vs WT +Fe control and only 79 and 235 differentially expressed gene IDs present at respectively TP A and TP B in *sufb-RNAi* +Fe vs WT +Fe control.

To visualize potential overlap and differences in DEGs due to either low Fe or loss of SufB we generated Venn diagrams (Figure 3). We first compared *sufb-RNAi* +Fe with WT +Fe control at both time point A and B to determine differential expression that is closely linked to the loss of *SUFB*. Only 47 common DEGs were shared across the time points, with 44 of these being up-regulated compared to WT +Fe control (S Figure 1). We then compared these 47 common DEGs due to loss of *SUFB* with transcriptome changes in WT -Fe treatment at both TP A and TP B. When differential expression was compared between WT -Fe treatment vs WT +Fe control and *sufb-RNAi* +Fe vs WT +Fe control, no DEGs were shared at TP A, and only the down-regulation of *SUFB* was shared at TP B between *sufb-RNAi* +Fe and WT -Fe treatment (Figure 3).

Because the transcriptional responses of WT -Fe treatment and *sufb-RNAi* +Fe were mostly distinct, we then sought to determine transcriptome changes specific to WT -Fe treatment (compared to WT +Fe control) and transcriptome changes specific to *sufb-RNAi* +Fe (compared to WT +Fe control).

**Transcriptional changes in WT -Fe treatment compared to WT +Fe control.** Differentially expressed genes in response to Fe deficiency were grouped by the functions of their gene products as listed in The Arabidopsis Information Resource (TAIR). At TP A, before *SUFB* is down-regulated, DEGs encoding kinases and transmembrane proteins constituted the largest functional categories being differentially expressed in the rosettes due to low Fe (Figure 4a). Of the transcripts that were up-regulated or down-regulated alongside *SUFB* at TP B in WT -Fe treatment vs WT +Fe control, the largest functional categories of differentially expressed gene products were transcription

factors (TFs), signaling components, ion homeostasis proteins, and redox homeostasis components (Figure 4b).

Among the transcripts that were differentially expressed in WT -Fe treatment many Fe responsive transcripts, commonly used as markers for Fe deficiency,<sup>74</sup> were differentially expressed at TP B (Figure 4b). Specifically, bHLH transcription factors that mediate root response to Fe deficiency (*PYE*, *bHLH100*, and *bHLH101*) were found to be up-regulated also in shoots compared to WT +Fe control with at least 4 fold induction, while mRNA encoding for Fe sequestration proteins, such as the predicted vacuolar Fe importer, *VTL1*, and Fe storage molecules, *Ferritins 1, 3, and 4* (*FER1*, *FER3*, *FER4*), were down-regulated compared to WT +Fe control by the same degree (Figure 4b).

The down-regulation of *SUFB* in TP B in WT -Fe treatment compared to WT +Fe control allowed us to identify transcripts that displayed down-regulation similar to that of *SUFB* as well as up-regulation, opposite of *SUFB*, during Fe deficiency. Interestingly, only one other transcript whose gene product is required for Fe cofactor assembly was differentially expressed on low Fe at TP B; *Urophorphyrin Methylase 1* (*UPM1*), required for siroheme biosynthesis. Within the WT -Fe treatment transcriptional response, we identified a set of ERF family transcription factors that are differentially expressed in WT -Fe treatment compared to WT +Fe control. After bHLH transcription factors the ERF transcription factor family was the most enriched among DEGs. We also identified a set of co-regulated CC-type Glutaredoxins (GRXS)<sup>75,76</sup> that were down-regulated in response to low Fe.

Ethylene Response Factor Transcription factors have recently been identified as regulating root Fe uptake during deficiency along with bHLH transcription factors deficiency.<sup>34-36</sup> The three ERF transcription factors that we found to be differentially expressed were ERF53, RA2.12, and CRF2 (Figure 4a, b, Figure 5). ERF53 which has previously been characterized as an early regulatory factor in abiotic stress<sup>77</sup> was up-regulated 2 fold in WT -Fe treatment by TP A compared to WT +Fe control (Figure 4a, visualized by Integrative Genome Viewer (IGV) Figure 5). However, *ERF53* was no longer differentially expressed at TP B (Figure 4a, b). Two other ERF transcription factors, *RA2.12* and *CRF2* were down-regulated by about 1.5 fold at TP B in WT -Fe treatment compared to WT +Fe control (Figure 4b, Figure 5).

A set of cytosolic GRXS that are known to be co-regulated by N status<sup>58,59</sup> were down-regulated in WT -Fe treatment compared to WT +Fe control (Figure 4b). Therefore, we aimed to determine if this set of co-regulated GRXS could be responsible for Fe sensing in leaves. To test this, we measured protein and transcript accumulation for chloroplast proteins known to be down-regulated 7 days after low Fe treatment<sup>24</sup> in an RNAi knockdown line of *grxs3/4/5/7/8*<sup>58,59</sup> grown on nutrient agar (Figure 6). When compared to the WT Fe deficiency response, the Fe deficiency response of *grxs3/4/5/7/8* did not differ, as *SUFB*, *FDX2*, and the Rieske component of the Cyt-*b<sub>6</sub>f* complex were all down-regulated at the transcript and protein level in *grxs3/4/5/7/8* on low Fe and PSaA was maintained. Therefore, *GRXS3/4/5/7/8* do not seem to be required in wild-

type abundance to mediate initial regulation of *SUF*B, *FDX*2, and the *Rieske* mRNA, which are regulated as part of a leaf Fe deficiency response.

**Transcriptional changes in *sufb*-RNAi +Fe compared to WT +Fe control.** At TP B only, *VTL*1, a vacuolar Fe importer, which is known to be down-regulated during Fe deficiency,<sup>78</sup> was up-regulated in *sufb*-RNAi +Fe compared to WT +Fe control (S. Figure 1). However, *VTL*1 up-regulation in *sufb*-RNAi +Fe compared to WT +Fe control was not consistent across TP A and TP B. Among the up-regulated transcripts at both TP A and TP B was *SUFA*, a candidate Fe-S cluster transfer protein (S. Figure 1). *SUFA* expression was induced by 4 fold at TP B. No other SUF pathway transcripts were differentially expressed. *SUFA* transcript levels were however stable in Fe deficiency (S. table 2), although *SUFA* protein accumulation does decrease.<sup>24,44</sup>

*SUFA* transcript was over expressed in *sufb*-RNAi +Fe compared to WT +Fe control whenever *SUF*B transcript was decreased, as visualized by read coverage generated from Integrated Genome Viewer (IGV; Figure 7a). We sought to investigate if this was conserved across other *SUF*B knockdown lines and knockdown lines for other components of the *SUF*BCD complex.<sup>55</sup> We also determined if the protein level of *SUFA* correlates to these transcript level changes. Interestingly, when we measured protein accumulation of *SUFA* via western blotting, *SUFA* protein was absent from induced *sufb*, *sufc*, and *sufd*-RNAi knockdown lines, and *SUF*B was decreased at the protein level in all *sufb*, *sufc* and *sufd* lines compared to WT as previously reported (Figure 7b<sup>55</sup>). We used qPCR to determine transcript level changes of *SUFA* in the induced *sufb*, *sufc* and *sufd* lines and saw similar results to our RNA-seq data, in which *SUFA* transcript was significantly up-regulated in all lines lacking components of the major Fe-S scaffold compared to WT +Fe control (Figure 7c). To determine if this up-regulation of *SUFA* is specific to loss of *SUF*B, we analyzed the transcript abundance of *SUF*B in the induced *sufb*, *sufc* and *sufd* knockdown lines. As previously reported, *SUF*B was only decreased in the *sufb*-RNAi knockdowns (Figure 7b, c<sup>55</sup>), suggesting that *SUFA* transcript accumulates as a result of a deficiency in the major scaffold of the *SUF* pathway.

We further investigated the role of *SUFA* in chloroplast Fe homeostasis, specifically in response to Fe deficiency. We deprived homozygous *sufa*-KO (Salk 147938C) plants of Fe on nutrient agar and compared the protein and transcript response to WT Fe deficiency. *sufa* maintained Fe regulation of the known chloroplast Fe markers, however, *sufa* accumulated more *Rieske*, *Cytb*<sub>6</sub>, and *FDX*2 proteins compared to WT at the protein level (Figure 8). No significant differences were seen at the transcript level between *sufa* and WT transcript changes. However, there was a trend for *sufa* to accumulate higher transcript levels of *FDX*2 and *RIESKE* (Figure 8).

**Early Fe deficiency in WT mainly targets chloroplast localized gene products.** Because chloroplast metabolism is a target of leaf Fe deficiency acclimation, we also analyzed gene product localization at TP A and TP B for up and down-regulated genes in WT -Fe treatment compared to WT +Fe control, using the GO

localization annotations from TAIR. At both TP A and TP B, the largest portion of both up-regulated and down-regulated gene products are targeted to the chloroplast, suggesting that chloroplast metabolism is an initial target of leaf Fe deficiency (Figure 9). Even with only 4 transcripts up-regulated at TP A, 75% of the encoded gene products were predicted or known to be localized to the chloroplast, while 23% of down-regulated gene products were annotated as localized to the chloroplast. After 26 h of Fe limitation (TP B), 38% of differentially regulated gene products were localized to the chloroplast compared to 26.8% localized to the cytoplasm (Figure 9).

**ERF, and bHLH transcription factors are predicted to regulate down-regulated chloroplast localized gene products during Fe deficiency acclimation.** To determine whether genes that are differentially expressed alongside *SUF*B in WT -Fe treatment share promoter elements, we analyzed promoter sequences of DEGs at TP B. We analyzed the promoters of DEGs that were up and down-regulated in WT -Fe treatment compared to WT +Fe control at TP B using AthaMap (Figure 10a).<sup>65</sup> Because bHLH and ERF transcription factors accounted for 7 of the 9 transcription factors that were differentially expressed in WT -Fe treatment compared to WT +Fe control in the RNA-sequencing, we focused on these families in our analysis of promoter regions. Of the up-regulated and down-regulated genes at TP B, all (100%) had at least one putative promoter binding site for ERF (Figure 10a). Comparatively, only 57% of down-regulated genes and 76% of up-regulated genes had at least one putative promoter bHLH binding site (Figure 10a). While other transcription factor families all had *cis* elements present in up and down-regulated gene promoters, predominately, transcription factors from ERF and bHLH families were differentially expressed in the RNA seq. We also investigated the promoters of the four up-regulated bHLH Fe related transcription factors, *PYE*, *bHLH*100, *bHLH*101, *bHLH*28, along with *BRUTUS*, the E3 ubiquitin ligase that is known to regulate Fe uptake and sequestration during deficiency. We found that for these 5 regulatory proteins, promoters contained putative ERF *cis* elements (data not shown). AthaMap also allows for determination of putative transcription factors that are predicted to bind promoter *cis* elements based on known binding sequences for specific transcription factors.<sup>65</sup> The ERF family had the highest number of transcription factors that were predicted to bind to *cis* elements in promoters of DEGs at TP B. 37 ERF transcription factors were predicted to bind to *cis* elements in promoters of down-regulated genes and 35 were predicted to bind to up-regulated genes (Figure 10a).

Specific bHLH and ERF transcription factor families have been linked to Fe deficiency regulation in roots.<sup>27</sup> To determine if *cis* elements predicted to bind bHLH and ERF are more commonly found in the promoters of the DEGs in the leaf Fe acclimation response, suggesting a higher probability of regulation by these transcription factor families, we analyzed *cis* element enrichment. We compared the probability of occurrence of bHLH and ERF *cis* elements in the promoters of TP B DEGs with the probability of bHLH and ERF *cis* element occurrence across the *Arabidopsis* genome. To determine if

genes encoding chloroplast localized proteins may be regulated preferentially by a specific class of transcription factor, we also analyzed enrichment in promoters of DEGs whose gene products are predicted to localize to the chloroplast. In promoters of DEGs up-regulated in WT -Fe treatment compared to WT +Fe control, there was a preference for bHLH *cis*-elements (Figure 10b). ERF *cis* elements were not enriched in promoters of up-regulated DEGs. These same patterns remained when only promoters of up-regulated chloroplast localized gene products were analyzed. Promoters of all down-regulated DEGs in WT -Fe treatment compared to WT +Fe control, were enriched for bHLH *cis* elements. However, promoters of down-regulated chloroplast localized gene products were enriched for both bHLH and ERF *cis* elements.

**Loss of Fe-S cluster production in shoots does not alter Fe acquisition.** Surprisingly, no known Fe deficiency related transcripts were differentially expressed in the *sufb-RNAi* +Fe rosettes even though *SUFB* was strongly downregulated (Figure 4). This suggests that the decrease in chloroplast Fe-S cluster production resulting from down-regulation of *SUFB* that also occurs early in Fe deficiency cannot be responsible for triggering transcriptional changes due to Fe deficiency in the leaf. To determine if other aspects of iron homeostasis were altered in *sufb-RNAi* +Fe, we also wanted to characterize general Fe homeostasis parameters in induced *sufb-RNAi* +Fe plants. To determine physiological changes in response to Fe deficiency we measured shoot Fe accumulation and root Fe reductase activity at TP C. We analyzed *sufb-RNAi* +Fe (*sufb2-2*) alongside a second inducible *sufb-RNAi* knockdown, *sufb1-12*, to account for any differences in knockdown alleles. Rosette Fe concentration was measured by elemental composition. No differences in rosette Fe accumulation were seen between induced *sufb-RNAi* lines and WT +Fe control, whereas Fe was significantly decreased in the rosettes of WT -Fe compared to WT +Fe as expected (Figure 11a). The regulation of root Fe acquisition in the WT and *sufb* plants was assayed by root ferric reductase chelate measurements (FRO activity). FRO activity was significantly up-regulated in WT -Fe treatment compared to WT +Fe control and *sufb-RNAi* +Fe lines across the week of Fe deficiency (Figure 11b, c). Therefore, shoot *SUFB* activity was not limiting for root FRO activity or shoot Fe accumulation (Figure 11a, b, c).

Most of the Fe used as a cofactor in photosynthesis is in proteins that function in electron transport downstream of PSII. To compare the effects of Fe deficiency as well as the effect of *SUFB* loss on photosynthetic electron transport, we analyzed the chlorophyll fluorescence parameter Flux Photosystem II ( $\phi$ PSII) an indication of efficiency of electron transport at TP C. We used chlorophyll fluorescence imaging because it has the advantage of measuring fluorescence across the entire rosette, allowing a spatial resolution. Both *sufb-RNAi* +Fe and WT -Fe treatment had a comparable decrease in  $\phi$ PSII relative to WT +Fe control indicative of decreased photosynthesis and this decrease was most pronounced in the youngest leaves (Figure 11d). Thus, Fe deficiency and lack in Fe-S cluster assembly did not present similar transcriptome changes in the rosettes

despite sharing similarities in photosynthetic electron transport chain protein accumulation and activity, and a comparable capacity to respond to systemic Fe deficiency and to up-regulate root Fe uptake of WT plants and *sufb-RNAi* lines.

## Discussion

**The transcriptional response to loss of chloroplast Fe-S cluster assembly and low Fe are distinct.** Because down-regulation of *SUFB* by inducible RNAi and Fe deficiency treatment resulted in a comparable expression level of *SUFB* protein and similar leaf symptoms at each of the sampling points (Figure 1), it was of interest to compare the transcriptomes for both treatments. Interestingly, the transcriptional response to acclimate the leaf to Fe deficiency was found to be distinct from the transcriptional response to loss of chloroplast Fe-S cluster assembly resulting from loss of *SUFB* (Figure 3). *Arabidopsis* *SUFB* has previously been proposed as an Fe sensor for plastid Fe homeostasis as its activity is stimulated by addition of Fe.<sup>42</sup> However, the *sufb-RNAi* +Fe line shared few transcriptomic changes with WT -Fe treatment when compared to WT +Fe control (Figure 3), suggesting there are distinct transcriptional responses for acclimation to Fe deficiency and changes in Fe utilization.

Previously published studies that have characterized genes and proteins required for the acclimation to Fe deficiency report mis-regulation of root FRO activity and IRT1 mediated Fe uptake. For example, loss-of-function mutants in the Iron Man/Fe Uptake Inducing Peptide (IMA/FEP) phloem mobile peptides in *Arabidopsis* presented Fe deficiency chlorosis when grown at normal Fe levels.<sup>79</sup> Further, IMA/FEP loss-of-function lines did not induce root FRO activity on sufficient or deficient levels of Fe compared to WT.<sup>79</sup> Over-expression lines of IMA1, and inducible over-expression FEP1 lines had up-regulation of Fe responsive bHLH transcription factors, *bHLH38*, *bHLH39*, *bHLH100*, and *bHLH101*, as well as Fe storage proteins, *FER1*, *FER3* and vacuolar Fe importers.<sup>79,80</sup> *Arabidopsis* mutants of Oligo-Peptide Transporter 3 (OPT3) which functions in systemic Fe deficiency signaling, over accumulate Fe in the shoots.<sup>81</sup> In the present study, *sufb-RNAi* +Fe did not alter root FRO activity to increase Fe reductase for Fe uptake (Figure 11), further supporting the presence of distinct responses in acclimation to leaf Fe deficiency and leaf Fe utilization.

On low Fe, the importance of the initial down-regulation of *SUFB* may well be to lower Fe-S cluster assembly which may be necessary for adjusting Fe protein biogenesis and perhaps photosynthetic output to Fe status, as loss of *SUFB* results in loss of photosynthetic electron transport proteins.<sup>55</sup> While the inducible *sufb-RNAi* knockdown was previously found to accumulate lower levels of Fe-S photosynthetic proteins, the corresponding transcripts for these proteins were not differentially expressed in our RNA-sequencing analysis (S. Table 2). Thus, we propose that the down-regulation of *SUFB* during Fe deficiency which is conserved from cyanobacteria to plants may help coordinate protein maturation by a decrease in Fe-S cluster availability with the down-regulation of Fe-S requiring photosynthetic electron transport proteins.

**Chloroplast localized gene products are early targets of Fe deficiency.** In WT -Fe treatment compared to WT +Fe control, 38% of both up-regulated and down-regulated gene products

co-regulated with *SUFB* at TP B (26 h after low Fe) are localized to the chloroplast (Figure 9). At TP A, 2 h after low Fe, 75% of up-regulated and 23% of down-regulated gene products are localized to the chloroplast. This suggests that alteration to chloroplast metabolism is an initial step in acclimating the leaf to low Fe. Interestingly, photosynthetic impairment is not detectable until 4 days after Fe limitation.<sup>24</sup> Chloroplast metabolism is adjusted to Fe deficiency much earlier than downstream effects on photosynthetic capacity. The down-regulation of *SUFB* may be an important part of this initial acclimation response to down-regulate chloroplast localized gene products.

#### ERF and bHLH transcription factors may regulate Fe deficiency transcriptional changes to chloroplast localized gene products.

Genes that are co-regulated in rosettes with *SUFB* early after Fe limitation are of special interest. A set of bHLH transcription factors have been well characterized in the up-regulation of root Fe uptake during Fe limitation.<sup>33</sup> Fe responsive bHLH transcription factors are expressed in the shoots as well,<sup>23,56,57</sup> *SUFB* does not have promoter *cis* elements for bHLH transcription factors,<sup>24</sup> suggesting a yet undiscovered regulatory system. We found enrichment of *cis* elements for bHLH transcription factors in DEGs of both up and down-regulated chloroplast localized gene products, while ERF *cis* elements were only enriched in DEGs of down-regulated chloroplast localized gene products (Figure 10). Enrichment of ERF *cis* elements has also been reported in early (6 h) differentially expressed genes in the acclimation of leaf Fe deficiency in *Glycine max* (Soybean;<sup>82</sup>).

We identified three ERF family transcription factors that were themselves differentially expressed in WT -Fe treatment compared to WT +Fe control (Figure 4, 5). ERF transcription factors are reported to respond to multiple abiotic stresses including hypoxia, osmotic stress, cold, and drought stress.<sup>83,84</sup> Regulatory pathways composed of multiple ERF transcription factors are able to integrate responses from multiple stimuli and ERF regulation may also depend on patterns of ERF expression as some ERF transcription factors are induced quickly and strongly while others may be induced later in a response or to a lesser extent.<sup>84</sup> These characteristics allow for dynamic responses to acclimate plant cells to multiple abiotic stresses.<sup>84</sup> In the present study, ERF53 was upregulated rapidly after transfer to low Fe (within 2 h) and dramatically (a fold change greater than 4x WT +Fe control). Transcripts for RA2.12 and CRF2 were delayed in their down-regulation, decreasing by 1.5x by 26 h after transfer to low Fe. This sequential expression of ERF transcription factors may be necessary for the regulation of the leaf Fe acclimation response.

ERF transcription factors have recently been linked to Fe deficiency.<sup>34–36</sup> Furthermore, it has been reported that ethylene related transcription factors help regulate the root Fe deficiency response.<sup>34,36</sup> Ethylene Insensitive 1 and Ethylene Insensitive Like 1-3 (EIN1, EIL3) were determined to stabilize FIT in the root Fe uptake response by directly screening for FIT interacting proteins.<sup>34</sup> More recently, two ERF transcription factors, ERF4 and ERF72 have been characterized in regulating both root and shoot responses to Fe deficiency in *Arabidopsis*.<sup>37,38</sup> Both loss of function ERF4 and ERF72 mutants presented increased IRT1 expression in the roots in the presence of Fe and maintained chlorophyll in the leaves in Fe deficient conditions.<sup>37,38</sup> Further, ERF72 and ERF4 directly interacted with the promoter of the

chlorophyll degradation gene, *AtCLH1*, suggesting that ERF4 and ERF72 positively regulate chlorophyll degradation in leaf acclimation to Fe deficiency. While ERF4 and ERF72 also negatively regulate IRT1, but ERF4 directly binds to the promoter of IRT1.<sup>37,38</sup> ERF4 and ERF72 were also recently found to suppress root Fe uptake by repressing the root proton pump in apple species. A higher expression of MbERF4 and 72 correlated with a Fe sensitive apple variety, while a low expression correlated with an Fe tolerant apple variety.<sup>36</sup> Moreover, the PAP/SAL1 retrograde signaling pathway which allows communication between chloroplast and nucleus and mitochondria and nucleus has recently been linked with ERF factors and ethylene signaling in Fe deficiency.<sup>85</sup> Mutants in the PAP/SAL1 pathway respond with increased Fe accumulation in roots and shoots, and an increased FRO2 and IRT1 gene expression. The increase in Fe uptake in the PAP/SAL1 mutant lines may be through PAP/SAL1 regulation of ERF1, as ERF1 was also determined to be over expressed in the mutants compared to WT.<sup>85</sup>

Fe responsive ERF family transcription factors have also been identified via gene expression changes. For instance, differential expression of ERF transcription factors was seen in the transcriptional analysis of *Arabidopsis* WT -Fe plants and also in *sp17* mutant plants, which are defective in up-regulation of Cu uptake under Cu deficiency and results in an Fe overload.<sup>35</sup> Some ERF family proteins we found to be down-regulated during low Fe in gene expression studies, suggesting Fe regulated ERF transcription factors may be regulated to stop driving the expression of specific targets.<sup>37,38,85</sup> Similarly, in the present study, ERF transcription factors, *CRF2* and *RA2.12*, expression at TP B was down-regulated compared to WT +Fe control (Figure 4, 5). The down-regulation of these ERF factors may result in repression of chloroplast localized transcripts. Constitutive expression of *RA2.12* resulted in enhanced stress responses.<sup>86</sup> CRF2 is important in cytokinin responses and cytokinin has been reported to negatively regulate the root Fe deficiency response.<sup>87</sup>

Conversely to regulation of *RA2.12* and *CRF2*, *ERF53* was up-regulated (>2 fold) at TP A (2 h after low Fe) but was not differentially expressed 24 hours later. ERF53 was reported to be important in early responses to salt and drought stress but was found to be rapidly degraded by the RGLG1/RGLG2 E3 ubiquitin ligases.<sup>77</sup> RGLG1/RGLG2 have also previously been proposed to regulate root and shoot Fe responses post-transcriptionally.<sup>44</sup> It is possible that *ERF53* is induced early in the leaf Fe deficiency response to initiate abiotic stress responses but then is degraded by RGLG1/RGLG2 as bHLH transcription factors are up-regulated to initiate later Fe specific acclimation.

#### Regulation of *SUFA* is dependent on integrity of *SUFBCD* scaffold.

One of the most up-regulated transcripts in *sufb-RNAi* +Fe was *SUFA* whose gene product is chloroplast localized (Figure 3, S. Figure 1). *SUFA* is a putative carrier protein that has capacity to either bind Fe or Fe-S clusters.<sup>53</sup> However, its biochemical role *in vivo* has not been determined. Unlike the components of the *SUFBCD* major scaffold, *SUFA* knockouts do not have a clear phenotype.<sup>53</sup> *sufA* is not vital for *SUF* Fe-S cluster assembly in *E. coli* either; the mutational loss of *sufA* in *E. coli* subject to iron deficiency was not lethal, whereas the mutational loss of other *suf* components in Fe deficient *E. coli* were lethal.<sup>88</sup>

Surprisingly, in the current study, the Arabidopsis *SUFA* transcript level increased by greater than 3 fold in knockdowns of the major scaffold proteins while *SUFA* protein accumulation was largely absent (Figure 7). While the overaccumulation of *SUFA* mRNA is not seen in Fe deficiency (S. table 2;<sup>24</sup>), the *SUFA* transcript levels are maintained while protein levels decrease.<sup>24,44</sup> Our data suggests that the regulation of *SUFA* during Fe deficiency may be a consequence of down-regulation of *SUFB* as an indirect result of Fe deficiency.

Interestingly, the *sufa* knockout had the same response to Fe deficiency as WT but accumulated more FDX, Rieske, and Cyt $f$  protein (Figure 8). This observation allows for a hypothesis on the biochemical function of *SUFA* in Fe-S cluster assembly. We propose that *SUFA* may act to sequester either Fe or Fe-S clusters to help coordinate Fe-S protein insertion with availability of Fe-S requiring proteins in the chloroplast (Figure 12). Under normal conditions when the major *SUF* scaffold is fully functional, *SUFA* may hold excess Fe or Fe-S clusters while the Fe-S requiring proteins are being translated and folded (Figure 12). When there is a deficiency in the major scaffold, for instance when *SUFB* is downregulated in WT -Fe, *SUFA* protein without cofactor bound becomes unstable and is degraded, but transcript remains high. When Fe is resupplied to a plant, *SUFA* protein can be rapidly translated while *SUFB* and chloroplast Fe-S containing proteins are recovered. In this case, the quick recovery of *SUFA* protein may serve to hold Fe until the major scaffold is recovered, or to hold new Fe-S clusters as photosynthetic proteins are recovered (Figure 12). Lack of *SUFA* in the knockdown may result in the plant producing more proteins that are a sink for chloroplast Fe-S clusters.

**Chloroplast Fe-S synthesis capacity affects intracellular Fe homeostasis.** The down-regulation of *SUF* Fe-S cluster assembly during Fe deficiency may be important for altering cellular Fe distribution for prioritization of Fe. The vacuolar Fe importer, *VTL1*, was up-regulated in *sufb-RNAi* +Fe at TP B compared to WT +Fe control (S Figure 1). *VTL1* is known to be down-regulated during Fe deficiency, possibly to decrease Fe sequestration in the vacuole (Figure 4;<sup>78</sup>). Because *sufb-RNAi* +Fe does not accumulate high levels of rosette Fe, most likely, the loss of *SUFB* results in lowered plastid Fe use which may, in turn, result in increased cytosolic Fe levels which could trigger the up-regulation of *VTL1* transcript in *sufb-RNAi* +Fe.

## Conclusions

Deficiency in Fe-S cluster assembly and lack of Fe cause similar defects in photosynthetic electron transport chain function and chloroplast protein accumulation. However, loss of Fe-S cluster assembly and lack of Fe did not present similar transcriptome changes in the short term. Overall, the transcriptional changes in *sufb-RNAi* +Fe were opposite that of WT -Fe treatment. However, *sufb-RNAi* +Fe displayed up-regulation of *SUFA* transcript but no *SUFA* protein over-accumulation, suggesting that regulation of *SUFA* is dependent on the integrity of the *SUFBCD* scaffold. Additionally, *sufb-RNAi* +Fe presented up-regulation of the vacuolar Fe transporter, *VTL1*. Overall, transcriptional changes in *sufb-RNAi* +Fe suggest that a lack of plastid Fe use may lead to alterations in intracellular Fe homeostasis.

## Conflicts of interest

There are no conflicts to declare.

## Acknowledgements

We would like to thank Dr. Tai Montgomery for his guidance in experimental design and analysis of the RNA-sequencing data. We would also like to thank Dr. Anireddy Reddy for his help in analysis of the RNA-sequencing data and Jessica Warren for her help in training G.K. on methods to assess RNA quality.

- 1 S. Merchant and M. R. Sawaya, *Plant Cell*, 2005, **17**, 648-63.
- 2 A. Tanaka and R. Tanaka, in *Advances in Botanical Research*, ed. B. Grimm, Academic Press Inc., London, 2019, 6, pp. 183–212.
- 3 N. M. Crawford and H. N. Arst Jr., *Annual Review of Genetics*, 1993, **27**, 115-146.
- 4 H. Takahashi, S. Kopriva, M. Giordano, K. Saito and R. Hell, *Annu. Rev. Plant Biol.*, 2011, **62**, 157-184.
- 5 N. Murthy, S. Ollagnier-de-Choudens, Y. Sanakis, S. E. Abdel-Ghany, C. Rousset, H. Ye, M. Fontecave, E. A. H. Pilon-Smiths and M. Pilon, *J. Biol. Chem.*, 2009, **284**, 18254-64.
- 6 K. Ravet and M. Pilon, *Antioxidants Redox Signal.*, 2013, **19**, 919-932.
- 7 A. Jain and E. L. Connolly, *Front. Plant Sci.*, 2013, **4**, 348.
- 8 J. Balk and T. A. Schaedler, *Annu. Rev. Plant Biol.*, 2014, **65**, 125-153.
- 9 P. M. Wood, *Eur. J. Biochem.*, 1978, **87**, 9-19.
- 10 G. Sandmann and P. Böger, *Plant Sci. Lett.*, 1980, **17**, 417-424.
- 11 S. Merchant and L. Bogorad, *EMBO J.*, 1987, **6**, 2531-2535.
- 12 A. Bovy, G. de Vrieze, L. Lugones, P. van Horssen, C. van den Berg, M. Borrias and P. Weisbeek, *Mol. Microbiol.*, 1993, **7**, 1047-1065.
- 13 M. D. Page, M. D. Allen, J. Kropat, E. I. Urzica, S. J. Karpowicz, S. I. Hsieh, J. A. Loo and S. S. Merchant, *Plant Cell*, 2012, **24**, 2649-2665.
- 14 D. J. Kliebenstein, R. A. Monde and R. L. Last, *Plant Physiol.*, 1998, **118**, 637-650.
- 15 F. Myouga, C. Hosoda, T. Umezawa, H. Iizumi, T. Kuromori, R. Motohashi, Y. Shono, N. Nagata, M. Ikeuchi and K. Shinozaki, *Plant Cell*, 2008, **20**, 3148-3162.
- 16 H. Yamasaki, S. E. Abdel-Ghany, C. M. Cohu, Y. Kobayashi, T. Shikanai, and M. Pilon, *Journal of Biological Chemistry*, 2007, **282**, 16369-16378.
- 17 H. Yamasaki, M. Hayashi, M. Fukazawa, Y. Kobayashi and T. Shikanai, *Plant Cell*, 2009, **21**, 347-361.
- 18 M. Bernal, D. Casero, V. Singh, G. T. Wilson, A. Grande, H. Yang, S. C. Dodani, M. Pellegrini, P. Huijser, E. L. Connolly, S. S. Merchant and U. Krämer, *Plant Cell*, 2012, **24**, 738–761.
- 19 G. E. Kroh and M. Pilon, *Int. J. Mol. Sci.*, 2020, **9**, 3395.
- 20 G. Vert, N. Grotz, F. Dédaldéchamp, F. Gaymard, M. Lou Guerinot, J. F. Briat and C. Curie, *Plant Cell*, 2002, **14**, 1223-1233.
- 21 N. J. Robinson, C. M. Procter, E. L. Connolly and M. Lou Guerinot, *Nature*, 1999, **397**, 694-697.
- 22 A. Laganowsky, S. M. Gómez, J. P. Whitelegge and J. N. Nishio, *J. Proteomics*, 2009, **72**, 397-415.
- 23 J. Rodríguez-Celma, I. Chun Pan, W. Li, P. Lan, T. J. Buckhout and W. Schmidt, *Front. Plant Sci.*, 2013, **4**, 276.
- 24 L. J. Hantzis, G. E. Kroh, C. E. Jahn, M. Cantrell, G. Peers, M. Pilon and K. Ravet, *Plant Physiol.*, 2018, **176**, 596-610.

- 25 A. G. Glaesener, S. S. Merchant and C. E. Blaby-Haas, *Front. Plant Sci.*, 2013, **4**, 337.
- 26 A. F. López-Millán, M. A. Grusak, A. Abadía and J. Abadía, *Front. Plant Sci.*, 2013, **4**, 254.
- 27 T. Kobayashi, *Plant Cell Physiol.*, 2019, **60**, 1440-1446.
- 28 T. Brumbarova, P. Bauer and R. Ivanov, *Trends Plant Sci.*, 2015, **20**, 124-133.
- 29 J. Jeong, A. Merkovich, M. Clyne and E. L. Connolly, *Curr. Opin. Plant Biol.*, 2017, **39**, 106-113.
- 30 E. P. Colangelo and M. Lou Guerinot, *Plant Cell*, 2004, **16**, 3400-3412.
- 31 M. Jakoby, H. Y. Wang, W. Reidt, B. Weisshaar and P. Bauer, *FEBS Lett.*, 2004, **577**, 528-534.
- 32 Y. Yuan, H. Wu, N. Wang, J. Li, W. Zhao, J. Du, D. Wang and H. Q. Ling, *Cell Res.*, 2008, **18**, 385-397.
- 33 F. Gao, K. Robe, F. Gaymard, E. Izquierdo and C. Dubos, *Front. Plant Sci.*, 2019, **10**, 6.
- 34 S. Lingam, J. Mohrbacher, T. Brumbarova, T. Potuschak, C. Fink-Straube, E. Blondet, P. Genschik and P. Bauer, *Plant Cell*, 2011, **23**, 1815-1829.
- 35 R. Kastoori Ramamurthy, Q. Xiang, E. J. Hsieh, K. Liu, C. Zhang and B. M. Waters, *Metallomics*, 2018, **10**, 1824-1840.
- 36 G. Zhang, W. Liu, Y. Feng, D. Li, K. Li, Q. Sun, L. Zhai, T. Wu, X. Zhang, X. Xu, Y. Wang and Z. Han, *Plant Cell Physiol.*, 2020, **61**, 699-711.
- 37 W. Liu, Q. Li, Y. Wang, T. Wu, Y. Yang, X. Zhang, Z. Han and X. Xu, *Biochem. Biophys. Res. Commun.*, 2017, **491**, 862-868.
- 38 W. Liu, N. J. U. Karemera, T. Wu, Y. Yang, X. Zhang, X. Xu, Y. Wang and Z. Han, *PLoS One*, 2017, **12**, e0186580.
- 39 O. Thimm, B. Essigmann, S. Kloska, T. Altmann and T. J. Buckhout, *Plant Physiol.*, 2001, **127**, 1030-1043.
- 40 A. Borlotti, G. Viganì and G. Zocchi, *BMC Plant Biol.*, 2012, **12**, 189.
- 41 T. Shikanai, P. Müller-Moulé, Y. Munekage, K. K. Niyogi and M. Pilon, *Plant Cell*, 2003, **15**, 1333-1346.
- 42 X. Ming Xu, S. Adams, N. H. Chua and S. G. Møller, *J. Biol. Chem.*, 2004, **280**, 6648-6654.
- 43 X. Liang, L. Qin, P. Liu, M. Wang and H. Ye, *Plant, Cell Environ.*, 2013, **37**, 780-794.
- 44 I. C. Pan, H. H. Tsai, Y. T. Cheng, T. N. Wen, T. J. Buckhout and W. Schmidt, *Mol. Cell. Proteomics*, 2015, DOI:10.1074/mcp.M115.048520.
- 45 J. Georg, G. Kostova, L. Vuorijoki, V. Schön, T. Kadowaki, T. Huokko, D. Baumgartner, M. Müller, S. Klähn, Y. Allahverdiyeva, Y. Hihara, M. E. Futschik, E. M. Aro and W. R. Hess, *Curr. Biol.*, 2017, **27**, 1425-1436.
- 46 E. A. H. Pilon-Smits, G. F. Garifullina, S. Abdel-Ghany, S. I. Kato, H. Mihara, K. L. Hale, J. L. Burkhead, N. Esaki, T. Kurihara and M. Pilon, *Plant Physiol.*, 2002, **130**, 1309-1318.
- 47 H. Ye, S. E. Abdel-Ghany, T. D. Anderson, E. A. H. Pilon-Smits and M. Pilon, *J. Biol. Chem.*, 2006, **281**, 8958-8969.
- 48 D. Van Hoewyk, S. E. Abdel-Ghany, C. M. Cohu, S. K. Herbert, P. Kugrens, M. Pilon and E. A. H. Pilon-Smits, *Proc. Natl. Acad. Sci. U. S. A.*, 2007, **104**, 5686-5691.
- 49 J. Balk and M. Pilon, *Trends Plant Sci.*, 2011, **16**, 218-226.
- 50 B. Touraine, J. P. Boutin, A. Marion-Poll, J. F. Briat, G. Peltier and S. Lobreau, *Plant J.*, 2004, **40**, 101-111.
- 51 T. Yabe, K. Morimoto, S. Kikuchi, K. Nishio, I. Terashima and M. Nakai, *Plant Cell*, 2004, **16**, 993-1007.
- 52 S. Schwenkert, D. J. A. Netz, J. Frazzon, A. J. Pierik, E. Bill, J. Gross, R. Lill and J. Meurer, *Biochem. J.*, 2010, **425**, 207-214.
- 53 T. Yabe and M. Nakai, *Biochem. Biophys. Res. Commun.*, 2006, **340**, 1047-1052.
- 54 S. Bandyopadhyay, F. Gama, M. M. Molina-Navarro, J. M. Gualberto, R. Claxton, S. G. Naik, B. H. Huynh, E. Herrero, J. P. Jacquot, M. K. Johnson and N. Rouhier, *EMBO J.*, 2008, **27**, 1122-1133.
- 55 X. Hu, Y. Kato, A. Sumida, A. Tanaka and R. Tanaka, *Plant J.*, 2017, **90**, 235-248.
- 56 T. A. Long, H. Tsukagoshi, W. Busch, B. Lahner, D. E. Salt and P. N. Benfey, *Plant Cell*, 2010, **22**, 2219-2236.
- 57 A. B. Sivitz, V. Hermand, C. Curie and G. Vert, *PLoS One*, 2012, **7**, e44843.
- 58 K. Patterson, L. A. Walters, A. M. Cooper, J. G. Olvera, M. A. Rosas, A. G. Rasmusson and M. A. Escobar, *Plant Physiol.*, 2016, **170**, 989-999.
- 59 L. A. Walters and M. A. Escobar, *Plant Signal. Behav.*, 2016, **11**, e1171450.
- 60 G. E. Kroh and M. Pilon, *Funct. Plant Biol.*, 2020, DOI:10.1071/FP19374.
- 61 X. Hu, M. T. Page, A. Sumida, A. Tanaka, M. J. Terry and R. Tanaka, *Plant J.*, 2017, **89**, 1184-1194.
- 62 D. Kim, B. Langmead and S. L. Salzberg, *Nat. Methods*, 2015, **12**, 357-360.
- 63 S. Anders, P. T. Pyl and W. Huber, *Bioinformatics*, 2015, **31**, 166-169.
- 64 H. Heberle, V. G. Meirelles, F. R. da Silva, G. P. Telles and R. Minghim, *BMC Bioinformatics*, 2015, **16**, 169.
- 65 C. Galuschka, M. Schindler, L. Bulow and R. Hehl, *Nucleic Acids Research*, 2007, **35**, D857-D862.
- 66 G. Toledo-Ortiz, E. Huq and P. H. Quail, *Plant Cell*, 2003, **15**, 1749-1770.
- 67 D. Hao, M. Ohme-Takagi and A. Sarai, *J. Biol. Chem.*, 1998, **273**, 26857-26861.
- 68 T. D. Schmittgen and K. J. Livak, *Nat. Protoc.*, 2008, **3**, 1101-1108.
- 69 M. K. Udvardi, T. Czechowski and W. R. Scheible, *Plant Cell*, 2008, **20**, 1736-1737.
- 70 E. A. H. Pilon-Smits, S. Hwang, C. M. Lytle, Y. Zhu, J. C. Tai, R. C. Bravo, Y. Chen, T. Leustek and N. Terry, *Plant Physiol.*, 1999, **119**, 123-132.
- 71 M. A. Grusak, *Planta*, 1995, **197**, 111-117.
- 72 K. Maxwell and G. N. Johnson, *J. Exp. Bot.*, 2000, **51**, 659-668.
- 73 E. M. Farré and S. E. Weise, *Curr. Opin. Plant Biol.*, 2012, **15**, 293-300.
- 74 S. A. Kim, I. S. LaCroix, S. A. Gerber and M. Lou Guerinot, *Proc. Natl. Acad. Sci. U. S. A.*, 2019, **116**, 24933-24942.
- 75 N. Rouhier, E. Gelhaye and J. P. Jacquot, *Cell. Mol. Life Sci.*, 2004, **61**, 1266-1277.
- 76 N. Gutsche, C. Thurow, S. Zachgo and C. Gatz, *Biol. Chem.*, 2015, **396**, 495-509.
- 77 E. J. Hsieh, M. C. Cheng and T. P. Lin, *Plant Mol. Biol.*, 2013, **82**, 223-237.
- 78 J. Gollhofer, R. Timofeev, P. Lan, W. Schmidt and T. J. Buckhout, *PLoS One*, 2014, **9**, e110468.
- 79 L. Grillet, P. Lan, W. Li, G. Mokkapati and W. Schmidt, *Nat. Plants*, 2018, **4**, 953-963.
- 80 T. Hirayama, G. J. Lei, N. Yamaji, N. Nakagawa and J. F. Ma, *Plant Cell Physiol.*, 2018, **59**, 1739-1752.
- 81 Z. Zhai, S. R. Gayomba, H. Il Jung, N. K. Vimalakumari, M. Piñeros, E. Craft, M. A. Rutzke, J. Danku, B. Lahner, T. Punshon, M. Lou Guerinot, D. E. Salt, L. V. Kochian and O. K. Vatamaniuk, *Plant Cell*, 2014, **26**, 2249-2264.
- 82 A. N. Moran Lauter, G. A. Peiffer, T. Yin, S. A. Whitham, D. Cook, R. C. Shoemaker and M. A. Graham, *BMC Genomics*, 2014, **15**, 702.
- 83 J. Mizoi, K. Shinozaki and K. Yamaguchi-Shinozaki, *Biochim. Biophys. Acta - Gene Regul. Mech.*, 2012, **1819**, 86-96.
- 84 Z. Xie, T. M. Nolan, H. Jiang and Y. Yin, *Front. Plant Sci.*, 2019, **10**, 228.
- 85 M. Balparda, A. Armas, G. Estavillo, H. Roschztardt, M. Pagani and D. Gomez-Casati, *Mol. Plant Biol.*, 2020, **102**, 323-337.
- 86 Y. Yao, R. J. He, Q. L. Xie, X. hai Zhao, X. mei Deng, J. bo He, L.

## Journal Name

## ARTICLE

1  
2  
3  
4  
5  
6  
7  
8  
9  
10  
11  
12  
13  
14  
15  
16  
17  
18  
19  
20  
21  
22  
23  
24  
25  
26  
27  
28  
29  
30  
31  
32  
33  
34  
35  
36  
37  
38  
39  
40  
41  
42  
43  
44  
45  
46  
47  
48  
49  
50  
51  
52  
53  
54  
55  
56  
57  
58  
59  
60

- Song, J. He, A. Marchant, X. Y. Chen and A. M. Wu, *New Phytol.*, 2016, **213**, 1667-1681.
- 87 M. Séguéla, J. F. Briat, G. Vert and C. Curie, *Plant J.*, 2008, **55**, 289-300.
- 88 F. W. Outten, O. Djaman and G. Storz, *Mol. Microbiol.*, 2004, **52**, 861-872.

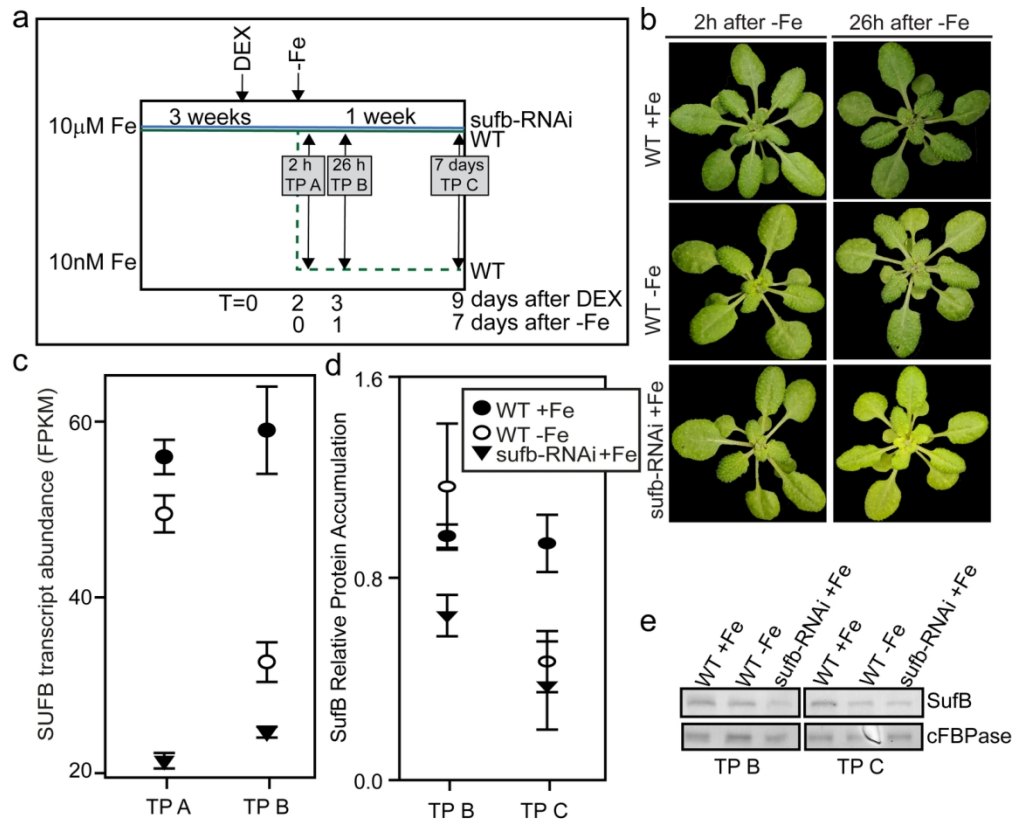


**Figure 1: Experimental Design and molecular characterization of plants for RNA-seq samples.** (a) Experimental set up and sampling times. Plants were grown on +Fe (10  $\mu$ M Fe(III)EDTA) for 3 weeks and WT plants were transferred to low Fe (10 nM Fe(III)EDTA) at 4 weeks of age. Plants were foliar sprayed with DEX 2 days prior to the start of WT -Fe treatment. Samples for RNA seq and protein were taken at 2 h (TP A) and 26 h (TP B) after the start of low Fe treatment. Physiological measurements were taken 7 days after the start of low Fe treatment (TP C) along with a second set of protein samples. (b) Representative images of WT +Fe control, WT -Fe treatment, and *sufb2-2* +Fe (*sufb-RNAi* +Fe) used for RNA-sequencing at TP A and TP B. (c) *SUFB* accumulation at transcript level at TP A and TP B. Each dot represents FPKM of *SUFB* and standard error. (d) Relative protein accumulation of *SUFB* at TP B and TP C (n=3). Each dot represents mean relative protein accumulation and standard error. (e) Representative immunoblots for *SUFB* at TP B and TP C used for protein quantification. cFBPase is presented as a loading control. Proteins were separated by SDS-PAGE (15% gel) and transferred to a 0.2  $\mu$ M pore nitrocellulose membrane (n=3-4).

134x110mm (300 x 300 DPI)

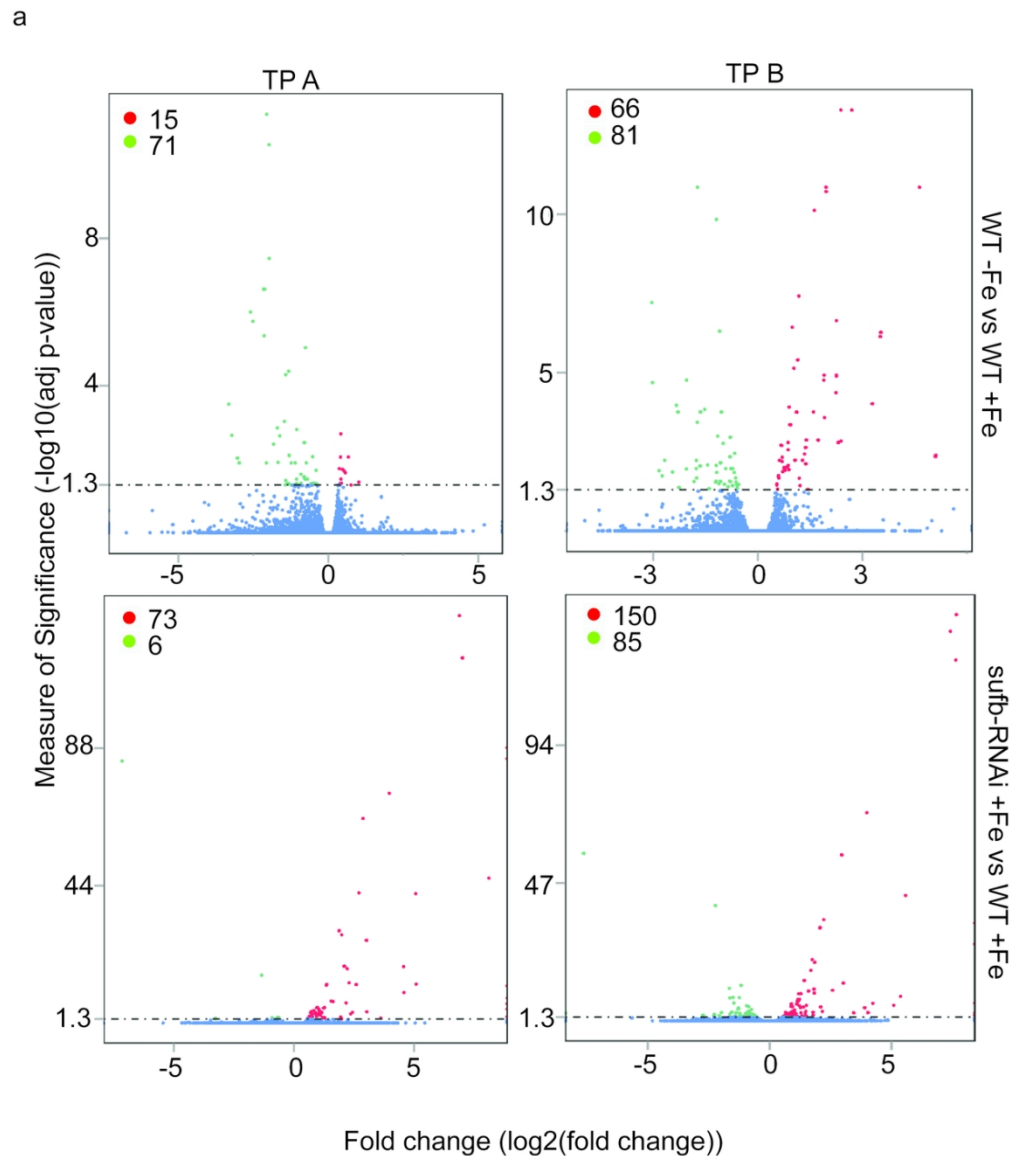


**Figure 2: Transcript abundance in WT -Fe treatment and *sufb-RNAi* +Fe at TP A and TP B.** Volcano plots of differentially expressed genes for WT -Fe treatment and *sufb2-2* +Fe (*sufb-RNAi* +Fe). Significance ( $-\log_{10}$  of the adjusted p-value) is plotted against  $\log_2$  Fold Change. Red dots represent up-regulated genes, green dots represent down-regulated genes, and blue dots represent unchanged genes. Down-regulated genes are those that are decreased in expression in WT -Fe treatment or *sufb-RNAi* +Fe compared to WT +Fe control; Up-regulated genes are these that have increased expression in WT -Fe treatment or *sufb-RNAi* +Fe compared to WT +Fe control.

105x121mm (300 x 300 DPI)



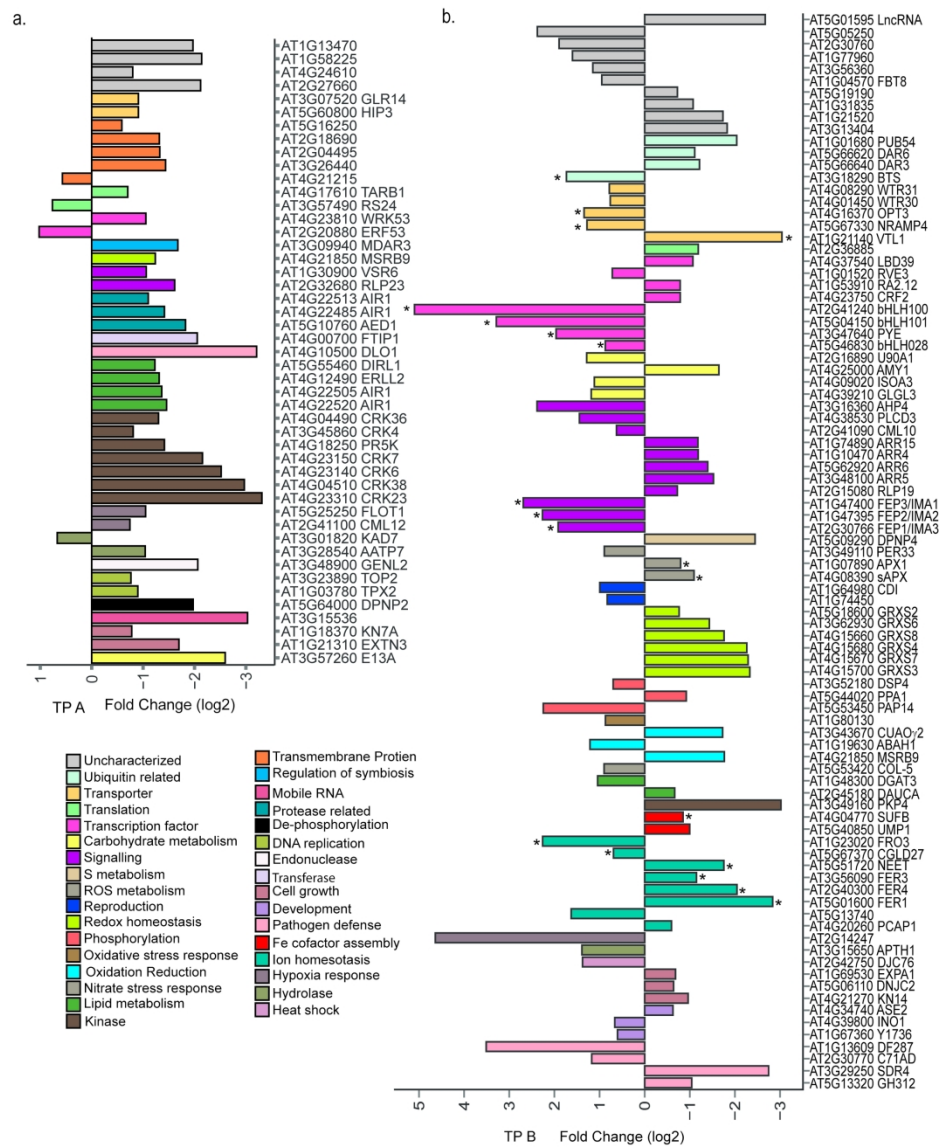


**Figure 4: Fold change of significant DEGs in WT -Fe treatment compared to WT +Fe control at (a) TP A and (b) TP B.** Log2 Fold Change is plotted for all DEGs in WT -Fe treatment. ATG numbers are listed on the right side of the graph. For genes that are annotated, the name of the gene is also included. Colors correspond to the TAIR annotated function of the gene product. Asterisks denote known Fe responsive transcripts.

210x246mm (300 x 300 DPI)

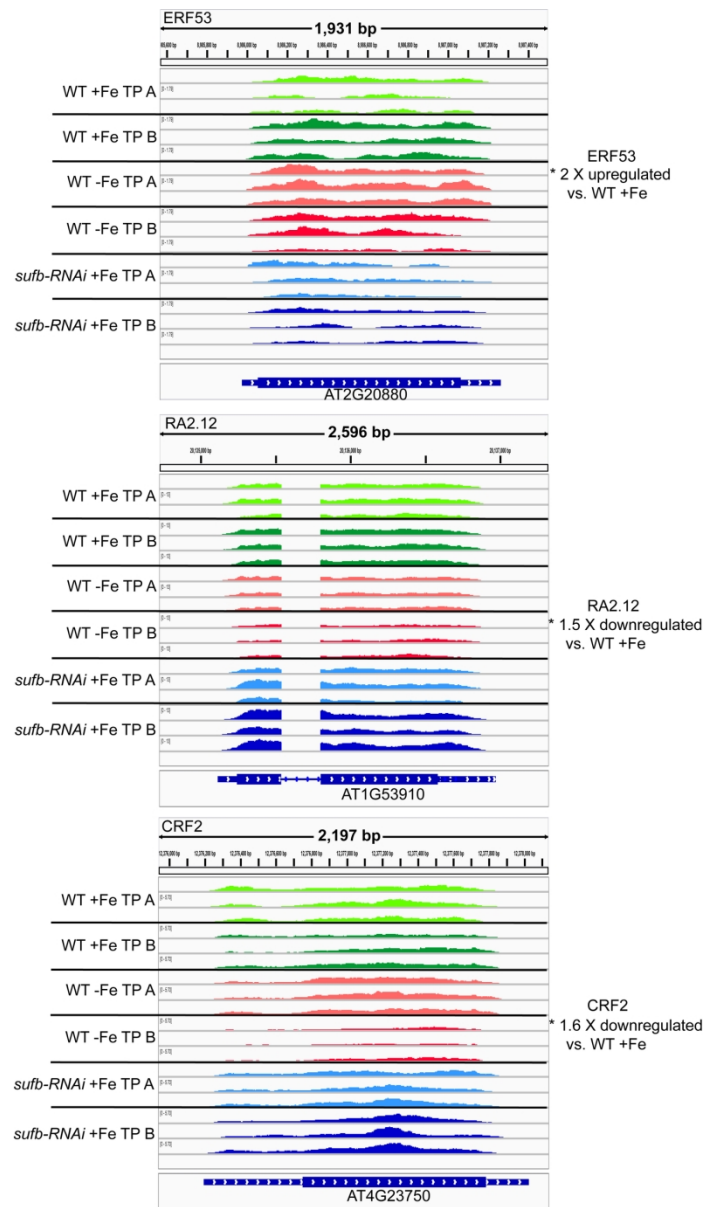


**Figure 5: Differential expression of 3 ERF family transcripts during Fe deficiency.** Read coverage of three biological replicates for *ERF53*, *RA2.12*, and *CRF2* in WT +Fe control, WT -Fe treatment, and *sufb*-RNAi +Fe (*sufb*-RNAi +Fe) by Integrative Genome Viewer (IGV). Height of peaks represents number of reads per area of the genome. Length of the genome area in view is denoted by number of base pairs above the read coverage. Location in genome is denoted by the ATG number at bottom of read coverage. Significant differential expression and fold change of the average FPKM compared to WT +Fe control is denoted to the right of the read coverage.

124x215mm (300 x 300 DPI)

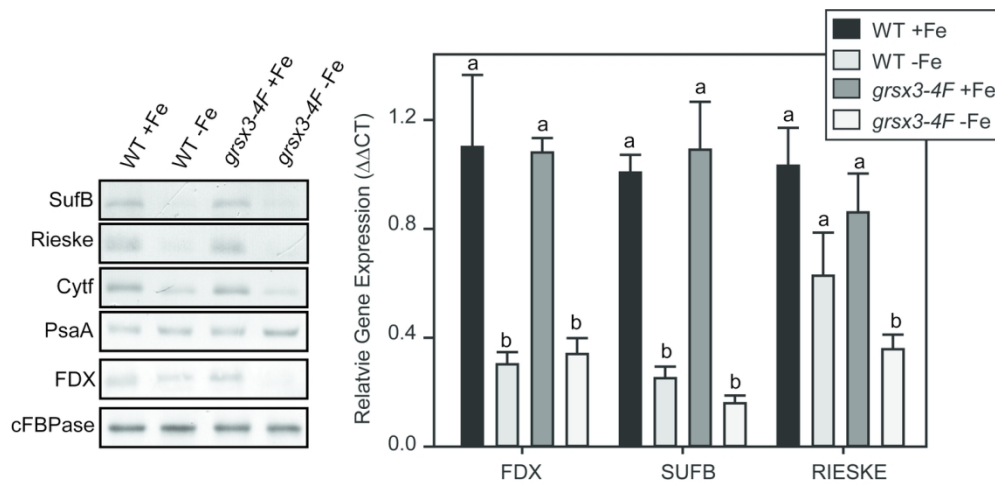


**Figure 6: Protein and transcript accumulation of photosynthetic Fe proteins in a *grxs3/4/5/7/8* knockdown line after 7 days of Fe deficiency.** (a) Protein and transcript accumulation of leaf proteins that are targeted during Fe deficiency (FDX, Cytf, Rieske, SUFB and PsaA) in WT and *grxs3/4/5/7/8*. Proteins were separated by SDS-PAGE (15% gel) and transferred to a 0.2 μM pore nitrocellulose membrane (n=4). cFBPase is included as a loading control. (b) Gene expression is measured by qRT-PCR. Transcript abundance is normalized to *UBQ10* and then to gene expression of WT (n=3).

136x65mm (300 x 300 DPI)

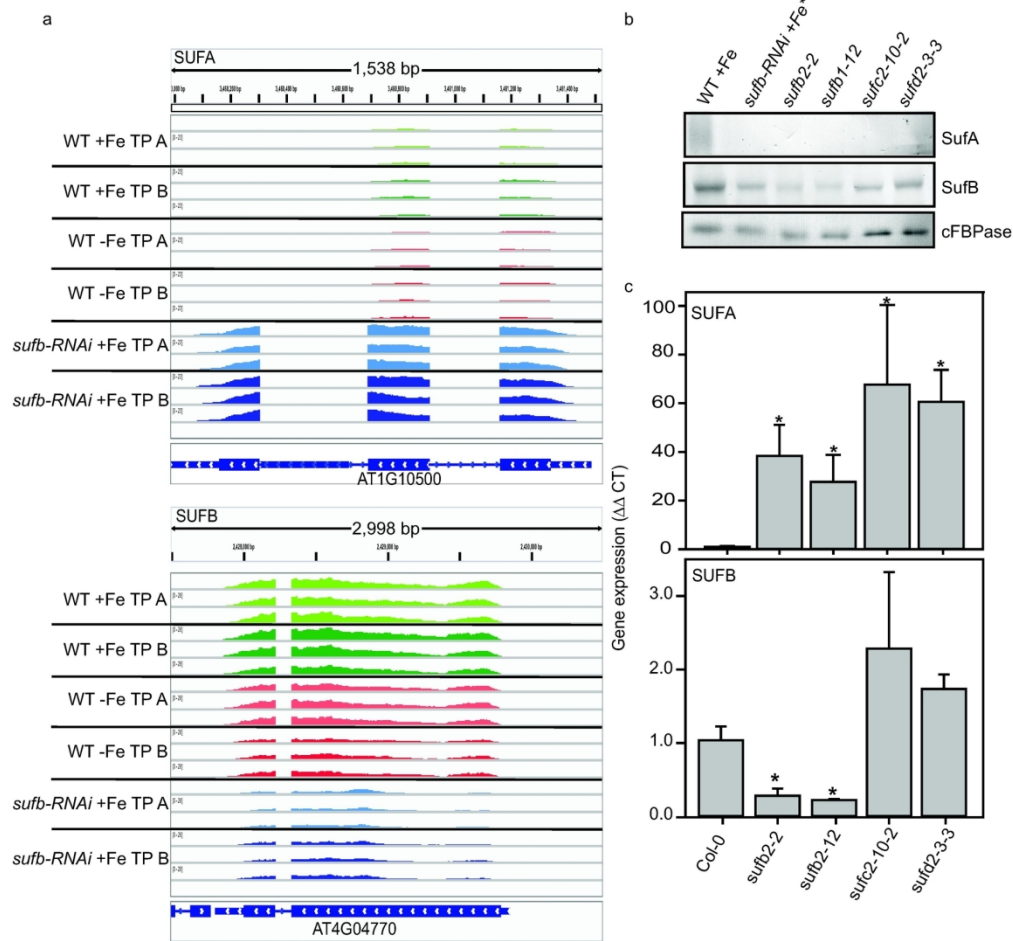


**Figure 7: SUFA protein and transcript accumulation in *sufb/c/d* knockdown lines.** (a) read coverage of *SUFB* and *SUFA* transcripts of 3 biological reps of WT +Fe control, WT -Fe and *sufb2-2* +Fe (*sufb-RNAi* +Fe) from IGV. Height of peaks represents number of reads per area of the genome. Length of the genome area in view is denoted by number of base pairs above the read coverage. Location in genome is denoted by the ATG number at bottom of read coverage. (b) protein accumulation of SUFA in *sufb/c/d* knockdowns compared to WT. Samples were taken 5 days after DEX induction. Asterisk denotes *sufb-RNAi* +Fe sample was taken from RNA-seq sampling. Representative blots of 3 reps are presented. Proteins were separated on a SDS-PAGE (15% gel) and transferred to a 0.2 μM pore nitrocellulose membrane and detected with indicated antibodies. (c) transcript abundance of *SUFA* and *SUFB* in *sufb/c/d* knockdowns analyzed by qPCR. Rosettes of knockout lines were collected 3 days after DEX treatment. Transcript abundance is normalized to *UBQ10* and then to abundance in WT (n=3). Significance was determined by an ANOVA and is denoted by an asterisk above the bar.

162x168mm (300 x 300 DPI)

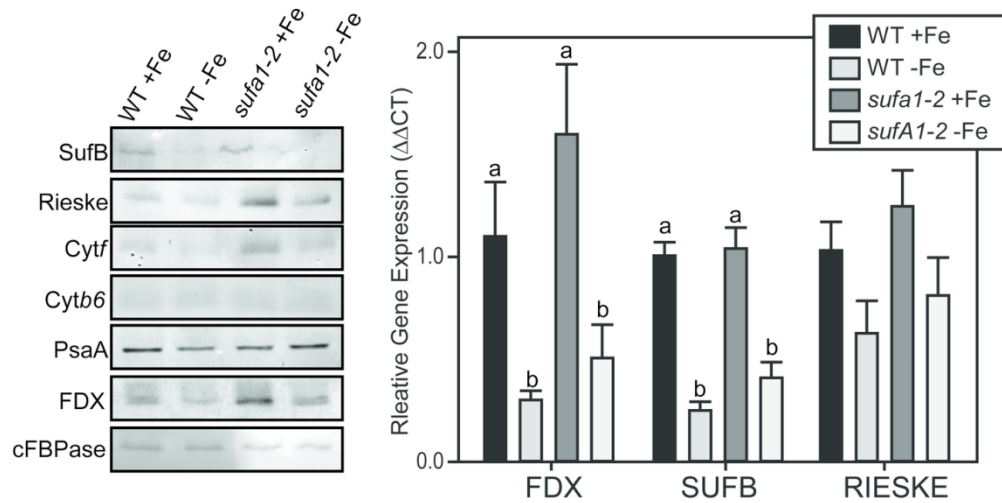


**Figure 8: Protein and transcript accumulation of photosynthetic proteins in *sufa* under normal and low Fe conditions.** Protein accumulation of Fe deficiency markers in WT and *sufa1-2* accumulated more FDX, Cytf, and Rieske in +Fe conditions compared to low Fe. Proteins were separated by SDS-PAGE (15% gel) and transferred to a 0.2  $\mu$ M pore nitrocellulose membrane (n=4). Gene expression of chloroplast Fe markers by qPCR. Transcript abundance is normalized to *UBQ10* and then to gene expression in WT (n=3). Significance was determined by an ANOVA and is denoted by letters above bars.

122x61mm (300 x 300 DPI)

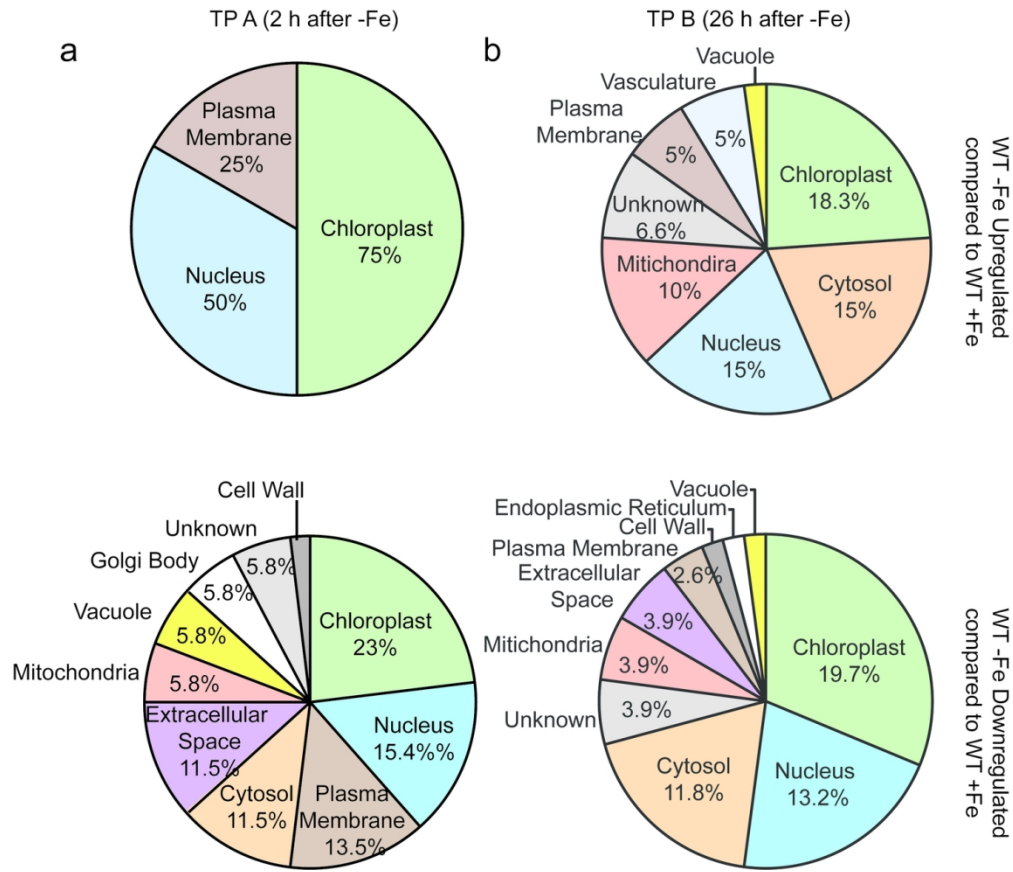


**Figure 9: Predicted sub-cellular location of gene products of differentially expressed genes.** (a) Predicted cellular location of gene products of DEGs at TP A for up and down-regulated DEGs in WT -Fe treatment. (b) Predicted cellular location of gene products of DEGs at TP B for up-regulated DEGs WT -Fe treatment. Only significantly differentially expressed genes with a fold change of at least 1.5 x higher or lower than WT +Fe control are represented. Down-regulated genes are those that are decreased in expression in WT -Fe treatment compared to WT +Fe control; Up-regulated genes are these that have increased expression in WT -Fe treatment compared to WT +Fe control.

126x109mm (300 x 300 DPI)

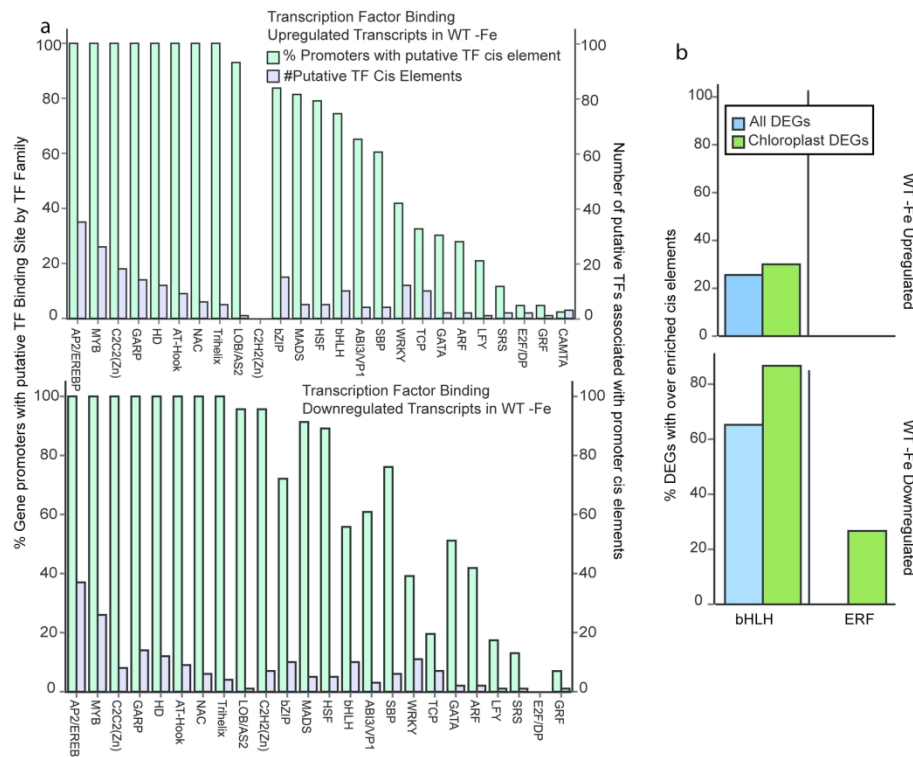


**Figure 10: Analysis of promoter *cis* elements for transcription factor binding in differentially expressed genes.** (a) Transcription factor family binding site enrichment in promoters of up-regulated and down-regulated genes in WT-Fe treatment analyzed using AthaMap. Green bars represent the percentage of differentially expressed genes that contain at least one putative transcription factor binding site for a specific transcription factor family. Purple bars represent the number of transcription factors within each family that are predicted by AthaMap to bind to promoter sequences of DEGs. (b) Percent of DEGs up and down-regulated that are enriched for *cis* elements of bHLH, and ERF Transcription factors in WT-Fe treatment.

Enrichment was analyzed for all DEGs and, separately, for DEGs of gene products localized to the chloroplast. Abundance of *cis* elements in promoters of DEGs was compared to the rate at which the same *cis* elements are found across the genome ( $p < 0.05$ ). Only significantly differentially expressed genes with a fold change of at least 1.5 x higher or lower than WT+Fe control are represented in both a and b. Abbreviations for transcription factor families are as follows: AP2/ERF: Apelata2/Ethylene Response Factor; MYB: MYB domain; C2C2(Zn): Cys2-Cys2 Zinc Finger; GARP: Golden2, ARR B, Psr1; HD: Homeodomain-leucine zipper; AT-Hook: glycine-arginine-proline motif; NAC: NAM, ATAF, and CUC; Trihelix: Three tandem helices; LOB/AS2: Lateral Organ Boundaries/Asymmetric Leaves 2; C2H2(Zn): Cys2-His2 zinc finger; bZIP: Basic Leucine Zipper; MADS: Minichromosome Maintenance1, Agamous, Deficiens, and Serum Response Factor; HSF: heat shock factors; bHLH: basic helix loop helix; ABI3/VP1: Abscisic acid insensitive1/Viviparous; SBP: Squamosa promoter Binding Protein family; WRKY: WRKYGQH heptapeptide containing; TCP: teosinte branched1, cycloidea, and PCF; GATA: bind (T/A)GATA(A/G) sequence; ARF: Auxin Response Factors; LFY: Leafy; SRS: Shi Related Sequence; E2F/DP: E2 promoter binding factor/Dimerization protein; GRF: Growth Regulating Factor; CAMTA: Calmodulin-binding transcription activator.

187x158mm (300 x 300 DPI)

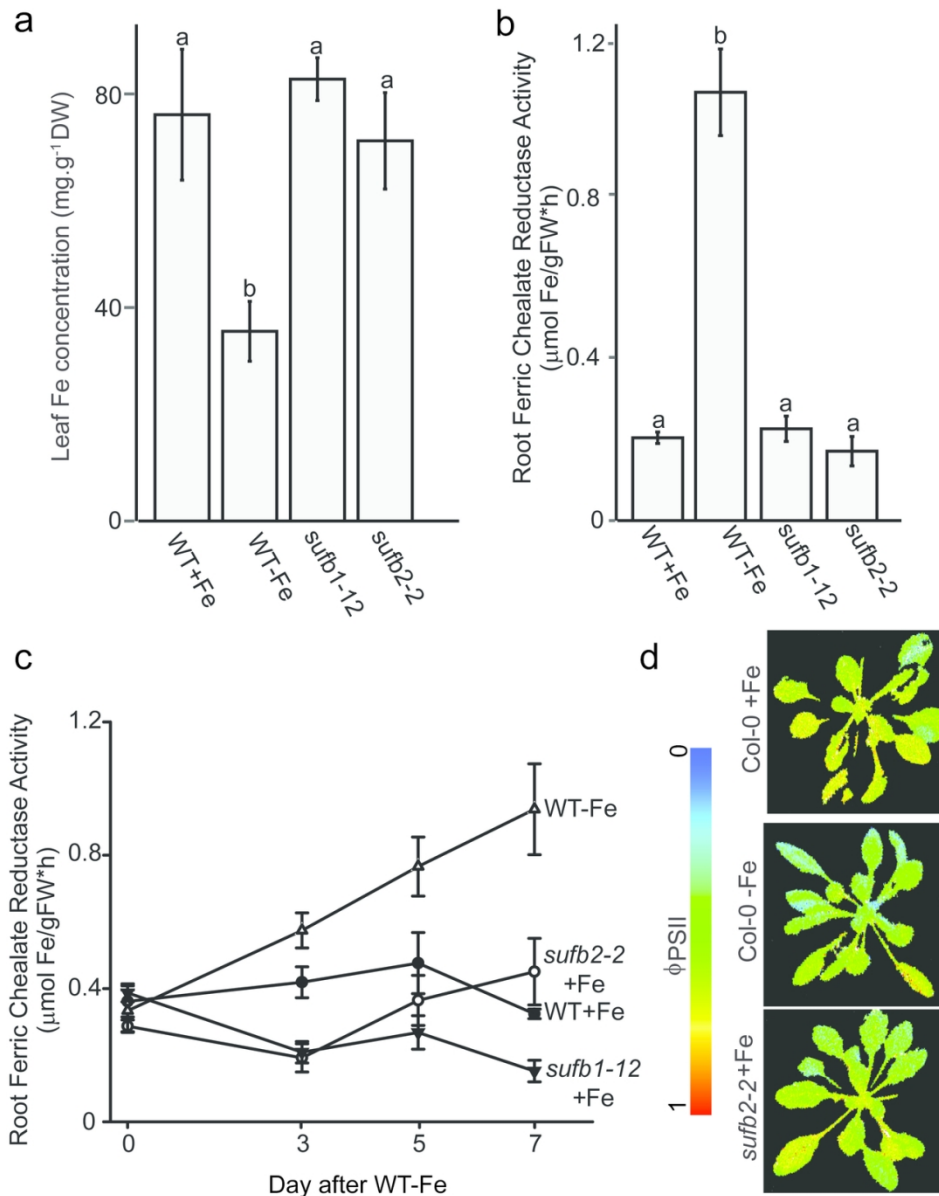


**Figure 11: Characterization of Fe homeostasis at TP C.** (a) Rosette Fe accumulation analyzed by ICP-OES in WT +Fe control, WT -Fe treatment, and two *sufb-RNAi* lines. Fe content was normalized to rosette dry weight (n=8). (b) Root ferric chelate reductase activity for WT +Fe control, WT -Fe treatment, and two *sufb-RNAi* lines at day 7 after Fe deficiency (n=5-10) and (c) across the week of Fe deficiency. Reductase activity was normalized by root fresh weight. Each bar represents mean and standard error. Significance was determined by an ANOVA and is denoted by a letter above bar. (d) False color images of chlorophyll fluorescence parameters,  $\Phi_{PSII}$ , indicative of electron transport downstream of PSII, for WT +Fe control, WT -Fe treatment and *sufb2-2* +Fe (*sufb-RNAi* +Fe). Red coloration correlates to higher  $\Phi_{PSII}$ , blue correlates to lower  $\Phi_{PSII}$

109x138mm (300 x 300 DPI)

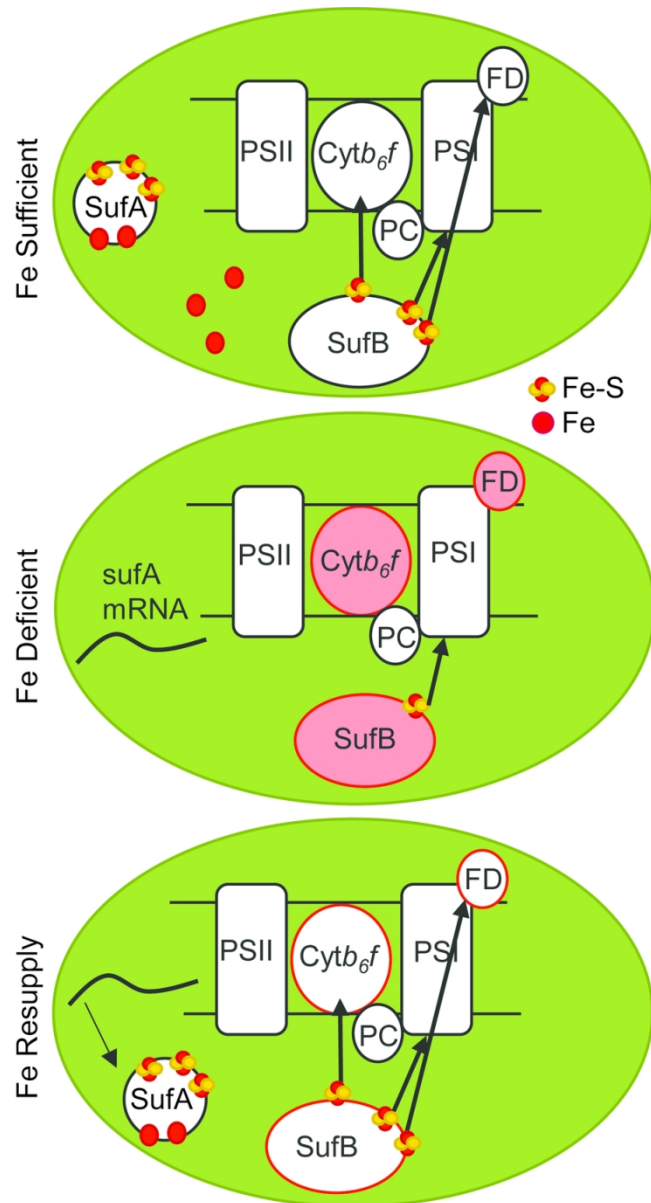


**Figure 12: Proposed model for SUFA as a buffer for Fe-S insertion into apo-proteins.** During Fe sufficient conditions, SUFBCD produces Fe-S clusters and they are inserted into apoproteins via Fe-S carrier proteins. SUFA may act to sequester excess Fe to be used in Fe-S assembly or excess Fe-S clusters to be inserted into proteins. During Fe deficiency, SUFB is down-regulated at the protein and transcript level resulting in less Fe-S clusters for proteins. *SUFA* transcript levels remain unchanged, but protein is degraded. In the hypothesized model, upon Fe resupply, as SUFB and Fe-S requiring proteins are recovering, *SUFA* can be quickly translated to hold excess Fe atoms or Fe-S clusters, thus providing buffering capacity as target Fe proteins again become expressed. Decreased protein levels are represented as ovals with a red outline, decreased transcript levels for the corresponding proteins are represented by red filled ovals. Black outlined symbols represent unchanged protein levels and white filled symbols represent unchanged transcript levels for the corresponding proteins.

77x145mm (300 x 300 DPI)

1  
2  
3  
4  
5  
6  
7  
8  
9  
10  
11  
12  
13  
14  
15  
16  
17  
18  
19  
20  
21  
22  
23  
24  
25  
26  
27  
28  
29  
30  
31  
32  
33  
34  
35  
36  
37  
38  
39  
40  
41  
42  
43  
44  
45  
46  
47  
48  
49  
50  
51  
52  
53  
54  
55  
56  
57  
58  
59  
60